J|A|C|S
ARTICLES
Published on Web 10/09/2002

Mechanism of the Addition of Nonenolizable Aldehydes and Ketones to (Di)metallenes ($R_2X{=}YR_2$, X = Si, Ge Y = C, Si, Ge): A Density Functional and Multiconfigurational Perturbation Theory Study

Nicholas J. Mosey, Kim M. Baines, and Tom K. Woo*

Contribution from the Department of Chemistry, The University of Western Ontario, London, Ontario, Canada, N6A 5B7

Received May 21, 2002

Abstract: The mechanism of the addition of nonenolizable aldehydes and ketones to group 14 (di)metallenes has been examined through a theoretical study of the addition of formaldehyde to Si=C, Ge=C, Si=Si, Si=Ge, and Ge=Ge bonds at the B3LYP/6-311++G(d,p) and CAS-MCQDPT2/6-31++G(d,p) levels of theory. The reaction pathways located can be grouped as either involving the formation of singlet diradical or zwitterionic intermediates or as concerted processes. Within each group of reaction pathways, several different mechanisms have been located, with not all mechanisms being available to all of the (di)metallenes. It was found that for reactions in which a Si−O bond results (i.e., addition to Si=C, Si=Si, and Si=Ge) both diradical and zwitterionic intermediates are possible; however, the formation of diradical intermediates was not found for reactions that result in the formation of a Ge−O bond (addition to Ge=C and Ge=Ge). The underlying cause of this pathway selectivity is examined, as well as the effect of solvent on the relative energies of the pathways. The results of the study shed light on the cause of experimentally obtained results regarding the mechanism of the reaction of (di)metallenes with nonenolizable ketones and aldehydes.

I. Introduction

The original syntheses of stable compounds containing multiple bonds involving heavier group 14 elements such as silicon[1,2] and germanium[3−5] resulted in a new and active area of chemical study. In the years since the discovery of these compounds, referred to throughout this paper as (di)metallenes[6], a great deal of experimental and theoretical effort has focused on examining the various reactions that they take part in.[7−22] The reactivity of these compounds may parallel that of their alkene analogues, and thus, an understanding of the underlying mechanisms of the reactions in which (di)metallenes participate is of considerable interest to a wide range of chemists. Unfortunately, few thorough investigations into the mechanisms of these reactions have taken place and mechanistic details are sparse in all but a few cases, such as the addition of alcohols and water to (di)metallenes.[23−27] To develop a better understanding of these compounds, in depth studies into the mechanisms of the reactions of (di)metallenes with various reagents are necessary.

Although there are some notable exceptions,[28] in general, nonenolizable ketones and aldehydes add to (di)metallenes to

* To whom correspondence should be addressed. E-mail: twoo@uwo.ca.

(1) Brook, A. G.; Abdesaken, F.; Gutekunst, B.; Gutekunst, G.; Kallury, R. K. *J. Chem. Soc., Chem. Commun.* **1981**, 191.
(2) West, R.; Fink, M. J.; Michl, J. *Science* **1981**, *214*, 1343.
(3) Couret, C.; Escudié, J.; Satgé, J. *J. Am. Chem. Soc.* **1987**, *109*, 4411.
(4) Meyer, H.; Baum, G.; Massa, W.; Berndt, A. *Angew. Chem., Int. Ed. Engl.* **1987**, *26*, 798.
(5) Masamune, S.; Hanzawa, Y.; Williams, D. J. *J. Am. Chem. Soc.* **1982**, *104*, 6136.
(6) In this study, we will use the generic label (di)metallene to refer to both metallenes and dimetallenes.
(7) Raabe, G.; Michl, J. In *The Chemistry of Organic Silicon Compounds*; Patai, S., Rappoport, Z., Eds.; Wiley: New York, 1989; p 1015.
(8) Müller, T.; Ziche, W.; Auner, N. In *The Chemistry of Organic Silicon Compounds*; Rappoport, Z., Apeloig, Y., Eds.; Wiley: New York, 1998; Vol. 2, p 857.
(9) Brook, A. G.; Brook, M. A. *Adv. Organomet. Chem.* **1996**, *39*, 71.
(10) West, R. *Angew. Chem., Int. Ed. Engl.* **1987**, *26*, 1201.
(11) Weidenbruch, M. In *The Chemistry of Organic Silicon Compounds*; Rappoport, Z., Apeloig, Y., Eds.; John Wiley and Sons, Ltd.: New York, 2001; Vol. 3, p 391.
(12) Okazaki, R.; West, R. *Adv. Organomet. Chem.* **1996**, *39*, 231.
(13) Weidenbruch, M. *Coord. Chem. Rev.* **1994**, *130*, 275.
(14) Escudié, J.; Ranaivonjatovo, H. *Adv. Organomet. Chem.* **1998**, *44*, 113.
(15) Baines, K. M.; Stibbs, W. G. *Adv. Organomet. Chem.* **1996**, *39*, 275.
(16) Escudié, J.; Couret, C.; Ranaivonjatovo, H.; Satgé, J. *Coord. Chem. Rev.* **1994**, *130*, 427.
(17) Barrau, J.; Escudié, J.; Satgé, J. *Chem. Rev.* **1990**, *90*, 283.
(18) Takahashi, M.; Veszpremi, T.; Hajgato, B.; Kira, M. *Organometallics* **2000**, *19*, 4660−4662.
(19) Takahashi, M.; Veszpremi, T.; Sakamoto, K.; Kira, M. *Molecular Physics* **2002**, *100*, 1703−1712.
(20) Hajgato, B.; Takahashi, M.; Kira, M.; Veszpremi, T. *Chemistry−A European Journal* **2002**, *8*, 2126−2133.
(21) Veszpremi, T.; Takahashi, M.; Hajgato, B.; Kira, M. *J. Am. Chem. Soc.* **2001**, *123*, 6629−6638.
(22) Kira, M.; Ishima, T.; Iwamoto, T.; Ichinohe, M. *J. Am. Chem. Soc.* **2001**, *123*, 1676−1682.
(23) Morkin, T. L.; Owens, T. R.; Leigh, W. J. In *The Chemistry of Organic Silicon Compounds*; Rappoport, Z., Apeloig, Y., Eds.; John Wiley and Sons, Ltd.: New York, 2001; Vol. 3, p 949.
(24) Morkin, T. L.; Leigh, W. J. *Acc. Chem. Res.* **2001**, *34*, 129.
(25) Leigh, W. J. *Pure Appl. Chem.* **1999**, *71*, 453.
(26) Sakurai, H. In *The Chemistry of Organic Silicon Compounds*; Rappoport, Z., Apeloig, Y., Eds.; John Wiley and Sons, Ltd: New York, 1998; Vol. 2, p 827.
(27) Wiberg, N.; Fischer, G.; Schurz, K. *Chem. Ber.* **1987**, *120*, 1605.
(28) In the addition of aromatic ketones, such as benzophenone, to silenes and germenes, the ketone can act as a 4π component to give a formal [4+2] cycloadduct.[7−9,14−16,29] In one case, the addition of formaldehyde to 1,1-dimethylsilene was reported to result in the formation of a siloxycarbene.[30] The addition of enolizable carbonyl compounds to dimetallenes (disilene,

10.1021/ja0269845 CCC: $22.00

Scheme 1. General Scheme for the Addition of Non-enolizable Ketones and Aldehydes to (di)Metallenes to Form (di)Metalloxetanes through Various Reaction Mechanisms

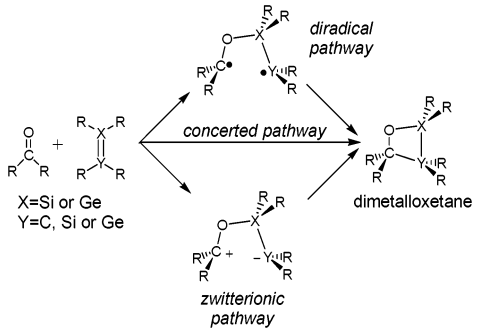

yield (di)metalloxetanes as shown in Scheme 1.[7−17,23−27,32−39] Metalloxetanes are of chemical interest as reactive intermediates because they undergo metathesis reactions. Such reactions are of synthetic value because they may provide an alternative of means of forming C═C and Y═C bonds, where Y is Si or Ge, as well as metallanones containing X═O bonds, where X is Si or Ge, which are also of significant chemical interest. As a result, metalloxetane formation has been the focus of several previous mechanistic studies that have led to the proposal of a variety of pathways for this addition including one-step concerted mechanisms and two-step processes involving progression through either zwitterionic or diradical intermediates as shown in Scheme 1.[23−26,40−49] The true nature of the mechanism for this reaction, and the factors influencing it, remain incompletely understood.

The formation of siloxetanes from the reaction of silenes ($R_2Si{=}CR_2$) with ketones in the presence of radical trapping agents has been previously studied in an attempt to differentiate between pathways involving the formation of diradical and zwitterionic intermediates.[46] The results showed that the formation of siloxetanes continued in the presence of the trapping agent and were taken as an indication that diradical formation does not occur along the reaction pathway. However, it is unlikely that the trapping agent (Bu_3SnH), at the concentration used, would be able to intercept a singlet diradical calling into question the significance of these results. Kinetic studies of the addition of acetone to silatrienes indicated that the reaction did indeed follow a stepwise pathway involving the initial attack of the silenic silicon atom by the carbonyl oxygen.[42] The results obtained were consistent with the formation of a diradical intermediate; however, the nature of the electronic structure of the species was not determined. Kinetic studies of the ene-addition of acetone to diphenylsilene are consistent with a stepwise mechanism involving the fast reversible formation of a zwitterionic silene−ketone complex followed by a rate-limiting proton transfer from the ketone to the silene.[40,43] The experimental evidence, in the case of silenes, thus suggests that the mechanistic pathway is very sensitive to the nature of the substituents.

Experimentally, the reaction involving the addition to germenes ($R_2Ge{=}CR_2$) has received less attention than the reaction with silenes; however, it is generally thought that both metallenes react along similar pathways.[25,41] Density functional theory calculations on the addition of carbonyl compounds to silenes and germenes with small substituents[50] have provided evidence that the additions to both compounds proceed along stepwise pathways instead of concerted ones; however, open-shell intermediates were not considered, and the possibility of a lower energy pathway involving the formation of a diradical intermediate persists.

The reaction of disilenes ($R_2Si{=}SiR_2$) and germasilenes ($R_2Si{=}GeR_2$) with aldehydes has been examined through the use of mechanistic probes specifically designed to differentiate between the formation of diradical and zwitterionic intermediates.[47,48] It was observed that the products formed from the reaction of both of these compounds with the probes were consistent with the formation of diradical intermediates. The application of the probes to the study of the addition of aldehydes to digermenes ($R_2Ge{=}GeR_2$) was examined,[49] and although the results obtained ruled out the possibility of the formation of a diradical intermediate it was not clear whether the reaction proceeded through a zwitterionic intermediate or followed a concerted pathway. It was proposed that the latter was more likely; however, this possibility was not examined further.

Thus, despite the fact that progress has been made in the attempt to elucidate the mechanism for the addition of nonenolizable ketones and aldehydes to (di)metallenes, the studies have been few and the results are not entirely conclusive. Lacking in these studies is a comprehensive examination of the potential energy surfaces for the addition of nonenolizable ketones and aldehydes to a variety of (di)metallenes through computational methods. In this paper, we present such an investigation by examining the addition of formaldehyde to a series of parent (di)metallenes (hydrogens as substituents) with computational methods capable of providing accurate descriptions of both open- and closed-shell systems. Our focus is on the examination of the potential energy surfaces leading to the formation of (di)-metalloxetanes.

The particular series of (di)metallenes examined in this study were silene, germene, disilene, germasilene, and digermene. Previous computational investigations of this reaction have taken

digermene, and germasilene) usually gives dimetalloxetanes although, recently, the formation of an ene-type adduct has been reported.[31] The analogous reaction with metallenes (silene and germenes) normally gives an ene-type product.

(29) Takeda, N.; Shinohara, A.; Tokitoh, N. *Organometallics* **2002**, *21*, 256.
(30) Trommer, M.; Sander, W.; Ottosson, C. H.; Cremer, D. *Angew. Chem., Int. Ed. Engl.* **1995**, *34*, 929.
(31) Lee, V. Y.; Ichinohe, M.; Sekiguchi, A. *Chem. Commun.* **2001**, 2146.
(32) Leigh, W. J.; Li, X. *Organometallics* **2002**, *21*, 1197.
(33) Schmohl, K.; Reinke, H.; Oehme, H. *Eur. J. Inorg. Chem.* **2001**, *2*, 481.
(34) Boomgaarden, S.; Saak, W.; Weidenbruch, M.; Marsmann, H. *Organometallics* **2001**, *20*, 2451.
(35) Lee, V. Y.; Ichinohe, M.; Sekiguchi, A. *Chem. Lett.* **2001**, *7*, 728.
(36) Wiberg, N.; Auer, H.; Wagner, S.; Polborn, K.; Kramer, G. *J. Organomet. Chem.* **2001**, *619*, 110.
(37) Eichler, B. E.; Powell, D. R.; West, R. *Organometallics* **1999**, *18*, 540.
(38) Wakita, K.; Tokitoh, N.; Okazaki, R.; Nagase, S.; von Schleyer, P.; Jiao, H. *J. Am. Chem. Soc.* **1999**, *121*, 11 336.
(39) Trommer, M.; Miracle, G. E.; Eichler, B. E.; Powell, D. R.; West, R. *Organometallics* **1997**, *16*, 5737.
(40) Bradaric, C. J.; Leigh, W. J. *Organometallics* **1998**, *17*, 645.
(41) Toltl, N. P.; Leigh, W. J. *J. Am. Chem. Soc.* **1998**, *120*, 1172.
(42) Leigh, W. J.; Sluggett, G. W. *Organometallics* **1994**, *13*, 269.
(43) Leigh, W. J.; Bradaric, C. J.; Sluggett, G. W. *J. Am. Chem. Soc.* **1993**, *115*, 5332.
(44) Sluggett, G. W.; Leigh, W. J. *J. Am. Chem. Soc.* **1992**, *114*, 1195.
(45) Toltl, N. P.; Leigh, W. J. *Organometallics* **1996**, *15*, 2554.
(46) Brook, A. G.; Chatterton, W. J.; Sawyer, J. F.; Hughes, D. W.; Vorspohl, K. *Organometallics* **1987**, *6*.
(47) Baines, K. M.; Dixon, C. E.; Samuel, M. S. *Phosphorus, Sulfur, Silicon Relat. Elem.* **1999**, *150*, 393.
(48) Dixon, C. E.; Hughes, D. W.; Baines, K. M. *J. Am. Chem. Soc.* **1998**, *120*, 11 049.
(49) Samuel, M. S. *Ph.D. Thesis, University of Western Ontario*, 2000.
(50) Khabashesku, V. N.; Kudin, K. N.; L., M. J. *Russ. Chem. Bull.* **2001**, *50*, 20.

place, however, they were of a limited nature, considering either the addition of formaldehyde to silene[51] or to two substituted silenes and germenes[50] without extensive examinations of the mechanism of product formation. To the best of our knowledge, no theoretical studies have examined the addition to disilene, germasilene, or digermene. This is also, to the best of our knowledge, the first study to consider the possibility of the formation of diradical intermediates and transition states in this reaction through theoretical methods.

The remainder of this paper is as follows: The computational methods are outlined in section IIa. Preliminary considerations regarding the computational methods employed are also discussed in section IIb. The results are presented and thoroughly discussed in section III, beginning with an examination of the structures of the reactants and products, followed by a description of all pathways located, an examination of solvent effects and a discussion of pathway availability. The pathways available to each (di)metallene are compared in section IV, and the conclusions are given in section V.

II. Methods

a. Computational Details. Density functional theory (DFT) calculations were performed with Becke's three parameter hybrid gradient-corrected exchange functional[52] and the gradient-corrected correlation functional of Lee, Yang, and Parr,[53] the B3LYP exchange correlation functional, using a 6-311++G(d,p) basis set with the Gaussian98[54] system of programs for the geometry optimizations of all reactants, products, intermediates and transition states. Calculations on the reactants, products, and closed-shell intermediates and transition states were performed with restricted DFT. Unrestricted DFT was employed to locate all singlet diradical intermediates and transition states with mixing of the HOMO and LUMO in the initial guess of the wave function to generate open-shell electronic structures. This practice results in spin-contamination of the wave function and the largest spin contaminant was projected out of all unrestricted calculations resulting in an S^2 eigenvalue of less than 0.035 in all cases. It should be exactly zero for a singlet. All DFT energies reported include unscaled zero point energy corrections. Frequency calculations were performed on all structures to confirm that the products, reactants and intermediates had no imaginary frequencies and that the transition states possessed only one imaginary frequency. Free energies at 298 K and 1 atm were obtained through thermochemical analysis performed along with the frequency calculations at the B3LYP/6-311++G(d,p) level with Gaussian98. Intrinsic reaction coordinate (IRC) calculations were performed at the B3LYP/6-311++G(d,p) level to confirm that all reported transition states do indeed lie between the intermediates and the products. Basis set superposition error was not corrected for. Wiberg bond orders[55] reported were calculated with the Natural Bond Order program[56] distributed with Gaussian98 and all spin densities reported are those determined through Mulliken population analysis[57] with Gaussian98.

Although DFT has been shown to provide qualitatively accurate results for calculations on singlet diradicals in some cases,[58−61] a proper treatment of such systems requires the use of multireference methods. Complete active space multi-configurational quadratic perturbation theory (CAS-MCQDPT2)[62,63] single-point calculations were performed on the B3LYP optimized geometries of all species in order to obtain an accurate description of the open-shell systems. This method provides an accurate description of the singlet diradical wave function through the inclusion of static correlation at the complete active space multi-configurational self-consistent field (CAS-MCSCF) level and dynamic correlation effects through second-order perturbation theory.

The CAS-MCQDPT2 calculations were performed with a 6-31++G-(d,p) basis set and all core, valence, and virtual orbitals were included in the correlation. The basis set convergence of the CAS-MCQDPT2 calculations was tested with the aug-cc-pVDZ[64] and the 6-311G++-(d,p) basis sets. (Larger basis sets could not be tested to due file size limitations with our computational resources.) Our tests revealed that the relative energies of the stationary points exhibited little variation with these three basis sets. The energies reported include a correction for the zero point energy equal to the values added to the B3LYP energies. The CAS-MCQDPT2 calculations were performed with the GAMESS suite of programs.[65]

The choice of the correct active space is crucial for multireference calculations. Upon completion of trial calculations with various active spaces, it was found that for the (di)metallene reactants it was necessary to use an active space with four electrons in four orbitals (4,4) consisting of the σ, σ^*, π, and π^* orbitals and an (8,6) active space including the σ, σ^*, π, and π^* orbitals and both oxygen lone pairs for formaldehyde. For the (di)metalloxetane products, the inclusion of the σ and σ^* orbitals for all bonds between heavy atoms as well as the inclusion of both oxygen lone pairs was found to be necessary, this yielded a (12,10) active space. For the diradical and zwitterionic intermediates and transition states, the σ and σ^* orbitals for all bonds between heavy atoms and both oxygen lone pairs were included, as well as the two singly occupied orbitals at the radical centers in the diradical species or the occupied and unoccupied lone pair orbitals on the ionic centers of the zwitterionic species. This also resulted in a (12,10) active space. A detailed description of the active space and reasons for the choice of active space used in the CAS-MCQDPT2 calculations can be found in the Supporting Information.

The orbitals used for the initial definition of the active space were obtained through single point Hartree−Fock calculations, with an unrestricted formalism being employed along with HOMO/LUMO mixing for the diradical species. Boys localization[66] of the occupied orbitals of the Hartree−Fock calculations and the use of the MVOQ[67] option in GAMESS, in which diagonalization of the Fock operator in the virtual space occurs along with the removal of several electrons from the system to give the virtual orbital's valence-like character, aided in the selection of the initial orbitals of the active space.

In cases where it was observed that there were large discrepancies between the B3LYP and CAS-MCQDPT2 energies, partial optimizations were performed at the CAS-MCQDPT2 level with the Trudge

(51) Bachrach, S. M.; Streitwieser, J. A. *J. Am. Chem. Soc.* **1985**, *107*, 1186.
(52) Becke, A. D. *J. Chem. Phys.* **1993**, *98*, 5648.
(53) Lee, C.; Yang, W.; Parr, R. G. *Phys. Rev. B* **1988**, *41*.
(54) Frisch, M. J.; Trucks, G. W.; Schegel, H. B.; Scuseria, G. E.; Robb, M. A.; Cheeseman, J. R.; Zakrewski, V. G.; Montgomery, J. A., Jr.; Stratmann, R. E.; Burant, J. C.; Dapprich, S.; Millam, J. M.; Daniels, A. D.; Kudin, K. N.; Strain, M. C.; Farkas, O.; Tomasi, J.; Barone, V.; Cossi, M.; Cammi, R.; Mennucci, B.; Pomelli, C.; Adamo, C.; Clifford, S.; Ochterski, J.; Petersson, G. A.; Ayala, P. Y.; Cui, Q.; Morokuma, K.; Malick, D. K.; Rabuck, A. D.; Raghavachari, K.; Foresman, J. B.; Cioslowski, J.; Ortiz, J. V.; Baboul, A. G.; Stefanov, B. B.; Liu, G.; Liashenko, A.; Piskorz, P.; Komaromi, I.; Comperts, R.; Martin, R. L.; Fox, D. J.; Keith, T.; Al-Laham, M. A.; Peng, C. Y.; Nanayakkara, A.; Gonzalez, C.; Challacombe, M.; Gill, P. M. W.; Johnson, B. G.; Chen, W.; Wong, M. W.; Andres, J. L.; Head-Gordon, M.; Replogle, E. S.; Pople, J. A. *Gaussian 98*, revision A.9; Gaussian, Inc.: Pittsburgh, PA, 1998.
(55) Wiberg, K. B. *Tetrahedron* **1968**, *24*, 1083.
(56) Glendening, E. D.; Reed, A. E.; Carpenter, J. E.; Weinhold, F. *NBO Version 3.1*.
(57) Mulliken, R. S. *J. Chem. Phys.* **1955**, *23*, 1833.
(58) Beno, B. R.; Wilsey, S.; Houk, K. N. *J. Am. Chem. Soc.* **1999**, *121*, 4816.
(59) Goldstein, E.; Beno, B. R.; Houk, K. N. *J. Am. Chem. Soc.* **1996**, *118*, 6036.
(60) Patterson, E. V.; McMahon, P. J. *J. Org. Chem.* **1997**, *62*, 4398.
(61) Worthington, S. E.; Cramer, C. J. *J. Phys. Org. Chem.* **1997**, *10*, 755.
(62) Nakano, H. *J. Chem. Phys.* **1993**, *99*, 7983.
(63) Nakano, H. *Chem. Phys. Lett.* **1993**, *207*, 372.
(64) Dunning, T. H., Jr. *J. Chem. Phys.* **1989**, *90*, 1007.
(65) Schmidt, M. W.; Baldridge, K. K.; Boatz, J. A.; Elbert, S. T.; Gordon, M. S.; Jensen, J. J.; Koseki, S.; Matsunaga, N.; Nguyen, K. A.; Su, S.; Windus, T. L.; Dupuis, M.; Montgomery, J. A. *J. Comput. Chem.* **1993**, *14*, 1347.
(66) Boys, S. F. *Quantum Science of Atoms, Molecule, and Solids*; Academic Press: New York, 1966.
(67) Bauschlicher, C. W., Jr. *J. Chem. Phys.* **1980**, *72*, 880.

Scheme 2. Thermodynamic Series Used to Calculate the X−O Bond Energies

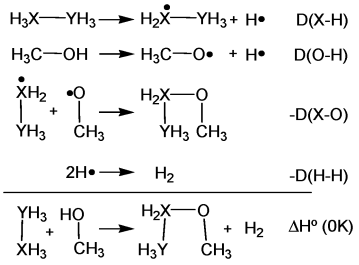

nongradient optimization method in GAMESS. The coordinates optimized in these partial optimizations were the X−Y, X−O, and C−O bond lengths. The active space and basis set used was the same as that described above.

It was necessary throughout the course of these calculations to evaluate the energies of the Si−O and Ge−O bonds. To determine the bond energies the series of thermodynamic reactions in Scheme 2 were used.

This series allows for the calculation of the X−O bond energies as follows

$$D(\mathrm{X{-}O}) = D(\mathrm{X{-}H}) + D(\mathrm{O{-}H}) - D(\mathrm{H{-}H}) - \Delta H^{\circ}(0\ \mathrm{K}) \quad (1)$$

Experimental data were used for all the values of D(X−H), D(O−H) and D(H−H). The values of D(X−H) used were 100.2,[68] 89.4,[68] and 83.0[69] kcal/mol for the C−H, Si−H, and GeH bonds, respectively. The values of D(O−H) and D(H−H) were 119.3[68] and 103.3[70] kcal/mol, respectively. The values of ΔH°(0 K) were calculated at the B3LYP/6-311++G(d,p) level. The choice of reagents, (di)metallanes and methanol, in this scheme were chosen to most closely represent the systems of interest, (di)metallenes and formaldehyde, while taking advantage of experimentally available values for D(X−H), D(O−H), and D(H−H). A test calculation was performed using ethane instead of a (di)metallane. Although experimentally the addition of aldehydes to ethene does not occur in the ground state and ethene was not considered as a reagent in this study, the use of ethane in the thermochemical scheme outlined above allowed for the calculation of the C−O bond energy and subsequent comparison to available experimental data. The results showed that the C−O bond energy, calculated with eq 1, was 92.6 kcal/mol which agrees reasonably well with the experimental value of 85.0 kcal/mol.

The effect of solvents on the energetics of the reaction were taken into account through the polarizable continuum model (PCM)[71−73] as implemented in Gaussian98. The solvents used were cyclohexane, acetone, acetonitrile, and water which allowed for the examination of a wide range of solvent polarity. The PCM calculations were performed at the B3LYP/6-311++G(d,p) level using the gas-phase geometries. The energies reported have zero-point corrections taken from the gas-phase calculations added to them. To check the validity of performing single-point calculations with the gas-phase geometries, we have performed full optimizations with acetone as a solvent for all structures along the diradical, zwitterionic, and concerted pathways for the addition of formaldehyde to silene. In general, we found extremely small geometric differences between the gas-phase and solvent optimized structures, with the largest discrepancy being the Si−O bond length of **ZW1−SiC-a** (vide infra) which was decreased by 0.34 Å in acetone when compared to the gas phase structure. All other bond lengths of this species remained relatively constant upon optimization with no changes in bond lengths greater than 0.01 Å. For all other stationary points along the three pathways, the largest differences in the bond lengths between the structures optimized in the gas phase and in acetone were less than 0.05 Å. The differences in the angles of all of the structures were less than 2.0° with the exception of the O−Si−C_1 and C_2−O−Si angles of the zwitterionic intermediate which were decreased by 5.2° and 6.1°, respectively, in acetone. Full optimizations also lead to negligible changes in the relative energies of the species. A comparison of the absolute energies of the species optimized in both the gas phase and in acetone revealed that the largest difference in energy was an increase of 1.0 kcal/mol for **ZW1−SiC-b**‡ (vide infra) when solvent was considered. The energy differences of all other species were less than 0.5 kcal/mol.

b. Preliminary Considerations Regarding Computational Methods. To test the validity of performing single point calculations at the multireference level on the DFT optimized geometries, selected structures were optimized at the CAS-MCSCF level, with the same basis set and active space as the CAS-MCQDPT2 calculations, and compared to the B3LYP geometries. The multireference methods provide a better description of the singlet diradical wave function than DFT,[74,75] and thus, the geometries of the open-shell systems optimized at the CAS-MCSCF level are considered to be more accurate. Our test calculations revealed that the B3LYP structures for the single-diradical intermediates and transition states were in excellent agreement with CAS-MCSCF optimized structures with bond lengths and angles between heavy atoms agreeing within 0.03 Å and 5° respectively. Because, the CAS-MCSCF calculations do not include dynamic correlation effects,[76] the B3LYP and CAS-MSCF geometries were also compared with partial geometry optimizations at the CAS-MCQDPT2 level. The CAS-MCQDPT2 calculations incorporate both dynamic and nondynamic correlation effects, however, the nongradient optimization used for the CAS-MCQDPT2 calculations only allows for partial optimization for systems of the size studied here, and does not allow for transition-state optimization. Partial geometry optimizations of selected open-shell systems at the CAS-MCQDPT2 level were also in excellent agreement with the DFT geometries with the bond lengths agreeing within 0.02 Å. Thus, the B3LYP optimized geometries were taken to be an accurate geometrical representation of the diradical structures.

Optimizations of the closed-shell species at the CAS-MCSCF level showed that the optimized structures were not in good agreement with the B3LYP results with bond lengths between heavy atoms differing by as much as 0.25 Å. The CAS-MCSCF approach is a more general form of the Hartree−Fock method, and in the limit that a system can be described by a single-reference wave function, the CAS-MCSCF method reduces to a Hartree−Fock calculation.[76] In all closed-shell species examined in this study, the ground-state determinant contributed an average of 95% of the total wave function, with its contribution ranging from 90% to 98% over all compounds, and thus, the closed-shell species can be said to be accurately represented by a single reference wave function.[77−79] For closed-shell molecules, DFT methods have been extensively tested against Hartree−Fock calculations and other accurate correlated methods for the prediction of reliable geometries and reaction profiles.[80,81] These studies show that DFT calculations are more accurate than HF calculations.

(68) Becerra, R.; Walsh, R. In *The Chemistry of Organic Silicon Compounds*; Rappoport, Z., Apeloig, Y., Eds.; John Wiley and Sons, Ltd.: New York, 1998; Vol. 2, p 153.
(69) Austin, E. R.; Lampe, F. W. *J. Phys. Chem.* **1977**, *81*, 1546.
(70) Huber, K. P.; Herzberg, G. *Constants of Diatomic Molecules*; Van Nostrand Reinhold: New York, 1979.
(71) Cossi, M.; Barone, V.; Cammi, R.; Tomais, J. *Chem. Phys. Lett.* **1996**, *255*, 327.
(72) Miertus, S.; Tomasi, J. *Chem. Phys.* **1981**, *55*, 117.
(73) Miertus, S.; Tomasi, J. *Chem. Phys.* **1982**, *65*, 239.
(74) Szabo, A.; Ostlund, N. S. *Modern Quantum Chemistry*; Macmillan Publishing Co., Inc.: New York, 1982.
(75) Klessinger, M.; Michl, J. *Excited States and Photochemistry of Organic Molecules*; VCH Publishers: Weinheim, 1994.
(76) Schmidt, M. W.; Gordon, M. S. *Annu. Rev. Phys. Chem.* **1998**, *49*, 233.
(77) Bone, R. G. A.; Pulay, P. *Int. J. Quantum Chem.* **1992**, *45*, 133.
(78) Bofill, J. M.; Pulay, P. *J. Chem. Phys.* **1989**, *90*, 3637.
(79) Pulay, P.; Hamilton, T. P. *J. Chem. Phys.* **1988**, *88*, 4926.
(80) Curtiss, L. A.; Redfern, P. C.; Raghavachari, K.; Pople, J. A. *J. Chem. Phys.* **2001**, *114*, 108.
(81) Lynch, B. J.; Truhlar, D. G. *J. Phys. Chem. A* **2001**, *105*, 2936−2941.

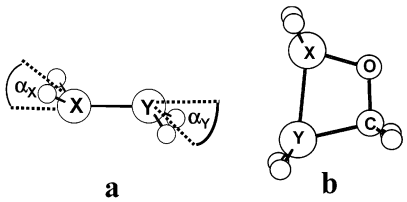

Figure 1. (a) Trans-bent geometry of (di)metallenes. α_X and α_Y denote the fold angles at atoms X(Si or Ge) and Y(C, Si or Ge), respectively. (b) General geometry of (di)metalloxetane products.

Because the B3LYP structures were in excellent agreement with the CAS-MCSCF and CAS-MCQDPT2 structures for the open-shell diradical complexes, and that there were large discrepancies between the B3LYP and CAS-MCSCF geometries for the closed-shell species (where DFT is known to perform better), it was decided that performing optimizations at the CAS-MCSCF level followed by single point calculations on those structures with CAS-MCQDPT2 would introduce greater error than performing single-point calculations on the B3LYP optimized geometries.

III. Results and Discussion

The geometries and energies of the reactants and products will be discussed first in parts a and b. This will follow with a description of the various reaction pathways found for these reactions in parts c and d. It was found that not all of the located pathways were available to all of the (di)metallenes studied. As a result, the discussion has been separated according to the various pathways located, with all participating (di)metallenes being discussed within the context of each mechanism. This allows for an increased facility in the comparison of the pathways, while minimizing the redundancy that would result from discussing each (di)metallene individually. This will follow with an examination of solvent effects in part e and a discussion of pathway selectivity in part f. In what follows, we have adopted a nonconventional naming system for the structures in order to accommodate the five (di)metallenes that we have examined as well as the three multistep reaction pathways (diradical, zwitterionic, concerted) that we have explored in each case. The three part naming scheme provides a description of the species and the nature of the reaction pathway where it is found. For example, **DR1-SiSi-b**, represents a disilene (X=Si, Y=Si) intermediate that lies on a diradical reaction pathway. The first part of the naming scheme refers to the nature of the reaction pathway—**DR** for diradical, **ZW** for zwitterionic, and **CN** for concerted. In many cases, we have located more than one unique diradical or zwitterionic pathway. Thus, the third numeric digit refers to the number of the unique pathway. For example, **DR1** refers to diradical pathway one, and **ZW3** refers to zwitterionic pathway three. The second part of the structure name refers to the (di)metallene involved, XY with X = Si, Ge, and Y = C, Si, Ge. Atoms X and Y are defined in Figure 1 with respect to the final (di)metalloxetane produced. The third part of the naming scheme is an alphabetic character that refers to the stationary point beyond the reactants toward the products. Thus, the "c" in **DR1-SiC-c**, reflects the fact that this is the third stationary point past the reactants that lies along the diradical pathway for the addition of silene (X = Si, Y = C) to formaldehyde. Finally, a superscript double dagger will denote that the species is a transition state structure.

a. Energies and Geometries of the Reactants. The geometries and electronic structures of (di)metallenes have been the focus of many previous investigations[82−86] which have shown that although they are ethene analogues, (di)metallenes do not necessarily possess a planar configuration in their most stable form. Instead, they may exhibit a trans-bent structure. This structure has the substituents above and below the molecular plane as defined by a planar geometry and is shown in Figure 1a. In the current study, geometry optimizations were performed on the parent (di)metallenes in an attempt to obtain both stable planar and trans-bent structures and allow for the subsequent comparison of the stabilities of the two geometries. It was observed that only planar structures were stable for silene and germene, whereas stationary points corresponding to both trans-bent and planar structures were located for disilene, germasilene, and digermene on the B3LYP potential energy surface. Relative energies derived from CAS-MCQDPT2 single-point calculations on B3LYP optimized geometries are also reported in Table 1.

Table 1. Selected Geometric Values and Energies[a] Relative to Planar Geometries for (di)Metallene Reactants

compd	X	Y	geometry	X–Y (Å)	α_X (°)	α_Y (°)	B3LYP	CAS[b]
Silene	Si	C	planar	1.708	0.0	0.0	0.0	0.0
Germene	Ge	C	planar	1.778	0.0	0.0	0.0	0.0
Disilene	Si	Si	planar	2.140	0.0	0.0	0.0	0.0
			trans-bent	2.173	30.8	30.8	−0.6	−2.4
Germasilene	Ge	Si	planar	2.180	0.0	0.0	0.0	0.0
			trans-bent	2.235	36.7	38.6	−1.9	−2.6
Digermene	Ge	Ge	planar	2.224	0.0	0.0	0.0	0.0
			trans-bent	2.305	42.9	42.9	−4.2	−2.6

[a] Energies reported are in kcal/mol. [b] CAS-MCQDPT2 single-point calculations on B3LYP optimized geometries.

Selected geometric values of the planar and trans-bent (di)-metallenes, as well as the energies relative to the planar reactants are given in Table 1. The energies show that the trans-bent structure is more stable than the planar one for disilene, germasilene, and digermene and that the stability of the trans-bent structure with respect to the planar one increases as heavier atoms become involved in the double bond. The magnitude of the fold angle also increases with this change. These results are consistent with those reported in the previous studies cited above and will not be discussed further.

b. Energies and Geometries of the Products. The geometries of the (di)metalloxetane products were optimized to compare their energies with those of the reactants, as well as examine the relative stabilities of possible isomers of the products. Restricting the search for stable products to oxetane analogues, the general structure of which is shown in Figure 1b, the products of the addition of formaldehyde to digermene and disilene can each only assume one stable isomer. On the other hand, for the addition to silene, germene, and germasilene it is possible to obtain two different products depending on the orientation of the (di)metallene with respect to the carbonyl group of formaldehyde. The geometries of all the products show that they are planar four-membered rings with dihedral angles between the atoms of the four-membered ring being no greater than 0.3°. Selected geometric values and the energies of the products relative to the sum of the energies of the separated reactants are given in Table 2.

(82) Grev, R. S.; Schaefer, H. F., III; Baines, K. M. *J. Am. Chem. Soc.* **1990**, *112*, 9458.
(83) Jacobsen, H.; Ziegler, T. *J. Am. Chem. Soc.* **1994**, *116*, 3667.
(84) Windus, T. L.; Gordon, M. S. *J. Am. Chem. Soc.* **1992**, *114*, 9559.
(85) Grev, R. S. *Adv. Organomet. Chem.* **1991**, *33*, 125.
(86) Trinquier, J. *J. Am. Chem. Soc.* **1990**, *112*, 2130.

Table 2. Calculated[a] Bond Lengths, Angles, and Relative Energies of the (di)Metalloxetanes

species		bonds(Å)				angles(°)			energies[b] (kcal/mol)	
X	Y	X–Y	X–O	Y–C	C–O	X–O–C	C–Y–X	Y–X–O	B3LYP	CAS[c]
Si	C	1.889	1.690	1.558	1.464	93.5	83.2	81.5	−49.8	−54.1
C	Si	1.908	1.458	1.908	1.458	104.3	74.1	90.9	−15.8	−18.3
Ge	C	1.978	1.838	1.553	1.452	93.9	85.6	75.5	−36.7	−49.8
C	Ge	1.998	1.447	1.997	1.447	106.2	70.8	91.5	−13.9	−20.0
Si	Si	2.343	1.695	1.942	1.461	107.1	72.1	79.8	−49.2	−41.3
Si	Ge	2.394	1.692	2.032	1.450	109.2	70.3	80.4	−42.5	−40.6
Ge	Si	2.393	1.850	1.933	1.450	106.0	102.9	74.6	−32.8	−35.1
Ge	Ge	2.447	1.847	2.023	1.438	107.9	72.5	77.2	−25.6	−35.7

[a] Geometries optimized at B3LYP/6-311++G(d,p) level. [b] Energy relative to the separated reactants. [c] CAS-MCQDPT2 single point calculations on B3LYP optimized geometries.

For the addition to both silene and germasilene, the products resulting from the formation of an Si−O bond are more stable than those resulting from the formation of a C−O or Ge−O bond, respectively, with the DFT and CAS-MCQDPT2 calculations in agreement. For the addition of formaldehyde to germene, the product resulting from the formation of a Ge−O bond is more stable than the product involving a bond between the germenic carbon and the carbonyl oxygen, once again with both methods in qualitative agreement. The observed lowest energy isomers agree with the experimentally observed products that show the existence of only siloxetanes and germasiloxetanes involving Si−O bonds[9,11] and germoxetanes with Ge−O bonds.[14]

The bond lengths and angles within the four-membered ring obtained for the siloxetane are in agreement with previously calculated structures.[51] The results are also in agreement with previously reported crystal structures,[46] with the exception of the C−C bond length, which is shorter by 0.12 Å in the calculated structures, which is likely due to the larger substituents, trimethylsilyl and adamantyl groups, on the experimental structures. For the germoxetane, the calculated values agree well with the crystallographic measurements on germoxetanes with bulky aromatic substituents.[87] Exceptions include the Ge−C bond length, for which the calculated value was approximately 0.10 Å shorter than that in the crystal structures, and the torsion angles between the heavy atoms in the four membered ring, which were ∼0° in the calculations that were on the order of 5° to 10° in the crystal structures. Once again, these differences likely result from the fact that no bulky substituents were included in the calculations. A comparison with the available crystal structures for disiloxetanes[35,36,88] shows excellent agreement with the largest discrepancy in bond lengths being less than 0.07 Å and all angles agreeing within 6°. These differences are small and likely result from differences in substituents. A comparison with an available, albeit disordered, germasiloxetane crystal structure[89] showed larger differences with bond lengths differing by as much as 0.12 Å and angles differing by as much as 10°. The crystal structure did exhibit disorder and these differences are likely an artifact of this disorder. The results still agree on a qualitative level. No reported crystal structures for digermoxetanes were found.

c. Open-Shell Pathways. Reaction pathways involving the formation of a singlet diradical intermediate were located for the addition of formaldehyde to silene, disilene and germasilene. The existence of such pathways is consistent with the previous experimental results.[42,46−48] For the other two (di)metallenes, germene and digermene, no stable diradical intermediates could be located. For the addition of formaldehyde to digermene, this result is also in agreement with experiment.[49] It should be noted that a structure possessing the electronic structure of a singlet diradical was located for the addition of formaldehyde to germene; however, this was not a stationary point on the B3LYP potential energy surface. Attempts to optimize this structure at the CAS-MCSCF level yielded a closed-shell structure, thereby providing further evidence that a stable diradical intermediate does not exist for the addition of formaldehyde to germene. The diradical pathway for the addition of formaldehyde to silene is unique and will be discussed first in part (i); the pathways for the addition to disilene and germasilene are similar to one another and will be discussed together in part (ii).

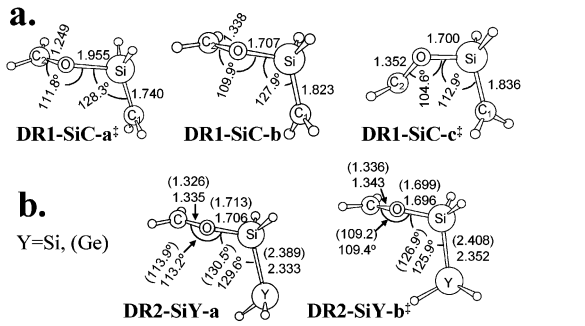

Figure 2. Geometries of intermediates and transition states along diradical pathway for the addition of formaldehyde to (a) silene and (b) disilene (Y = Si) and germasilene (Y = Ge). Parenthetic parameters in (b) are for the addition of germasilene. Bond lengths are in angstroms and angles are in degrees.

c(i). Addition to Silene through a Diradical Intermediate. For the addition of formaldehyde to silene a pathway involving the initial progression of the reactants through a transition state, **DR1-SiC-a‡**, to form a singlet diradical intermediate, **DR1-SiC-b**, followed by progression over another transition state, **DR1-SiC-c‡**, to form products was located. IRC calculations have been performed that confirm that the transition states link the intermediate to the reactants and products. These transition states and intermediates are shown in Figure 2a, whereas the energies along the potential energy surface relative to the reactants are given in Table 3.

A singlet diradical is characterized by possessing two unpaired electrons with opposite spin. Included in Table 3 are two metrics for providing the number of unpaired electrons in the species to determine the diradical character of the electronic structure.

(87) Lazraq, M.; Couret, C.; Escudie, J.; Satge, J. *Organometallics* **1991**, *10*, 1771.
(88) Schaefer, A.; Weidenbruch, M.; Pohl, S. *J. Organomet. Chem.* **1985**, *282*, 305.
(89) Baines, K. M.; Cooke, J. A.; Vittal, J. J. *Heteroatom Chem.* **1994**, *5*, 293.

Table 3. Energies, Spin Densities and HOMO/LUMO Occupations along Diradical Pathway for the Addition of Formaldehyde to Silene, Disilene, and Germasilene

	energy[a]			net spin[b]		occupations[c]	
species	B3LYP	CAS[d]	ΔG[e]	Y	C_2	HOMO	LUMO
			silene				
DR1-SiC-a‡	5.5	6.9	15.5	−0.33	0.31	1.95	0.07
DR1-SiC-b	2.0	−0.3	11.5	−0.96	0.92	1.22	0.79
DR1-SiC-c‡	3.6	−1.8	14.0	−0.96	0.90	1.37	0.64
			disilene				
DR2-SiSi-a	−4.9	−4.9	4.8	−0.86	0.92	1.24	0.76
DR2-SiSi-b‡	−4.0	−4.7	6.2	−0.91	0.95	1.22	0.78
			germasilene				
DR2-SiGe-a	−5.6	−5.6	4.2	0.73	−0.86	1.28	0.73
DR2-SiGe-b‡	−4.8	−6.4	5.5	0.78	−0.91	1.25	0.76

[a] Energies relative to sum of separated reactants reported in kcal/mol. [b] B3LYP 6-311G++(d,p) Mulliken populations. Positive values represent α spin, negative values represent β spin. [c] CAS-MCQDPT2 HOMO/LUMO natural orbital occupations obtained from a single point calculation on B3LYP optimized geometry. [d] CAS-MCQDPT2 single point calculations on B3LYP optimized geometries. [e] Gas phase relative free energy at 298 K and 1 atm at the B3LYP 6-311++G(d,p) level.

The first are the Mulliken net spin densities at both carbon atoms from the B3LYP calculations, which indicate the number of unpaired electrons at those sites. A singlet diradical would have an approximate net α spin density of one and a net β spin density of one, whereas a closed-shell species would have no net spin density. The second metric are the HOMO/LUMO occupations from the CAS-MCQDPT2 calculations that allow for an examination of the number of electrons in each of these orbitals. A singlet diradical will have occupation numbers of approximately one in each of these orbitals corresponding to each unpaired electron.[76,84] In contrast, a closed shell intermediate, such as a zwitterionic intermediate, there would be a HOMO occupation of 2.0 and a LUMO occupation of 0.0.

Formation of the diradical intermediate from the separated reactants requires the reaction to progress over an energy barrier corresponding to the transition state species **DR1**−**SiC-a**‡. As depicted in the structure of **DR1**−**SiC-a**‡ shown in Figure 2a, the carbonyl oxygen of the formaldehyde complexes with the π-system of the Si═C bond through its n-orbital plane. Several other orientations of interaction between the formaldehyde molecule and the silene were examined, however, only one diradical pathway could be located. The B3LYP results show the value of this barrier to be 5.5 kcal/mol with the CAS-MCQDPT2 result in agreement showing a barrier of 6.9 kcal/mol. The free energy of this species relative to that of the reactants is 15.5 kcal/mol, a large portion of which is due to an entropic contribution resulting from complexation. Analysis of the net spin density on the radical centers and the HOMO/LUMO occupations reveals that **DR1**−**SiC-a**‡ has an electronic structure between the approximately closed-shell reactants and the open-shell singlet diradical intermediate. The net Mulliken spins given in Table 3 show a small build-up of spin density centered on Y═C_1 and C_2. An isosurface plot of the net spin density shown in Figure 3a, also reveals the spin polarization localized at the two carbon centers.

The intermediate, **DR1**−**SiC-b**, involves the formation of an Si−O single bond along with rotation of the carbonyl group relative to the (di)metallene. The Si−O bond in the intermediate **DR1**−**SiC-b**, is 1.71 Å which is essentially the bond distance of 1.69 Å in the final siloxetane product showing that a Si−O single bond has completely formed in the diradical intermediate. This is corroborated by the calculated Si−O bond order of 0.56 compared with that of 0.64 in the products. Analysis of the net spin densities shows a net spin corresponding to roughly one unpaired electron at each of the radical centers and the CAS-MCQDPT2 HOMO/LUMO occupations indicate that each of these orbitals are occupied by approximately one electron. Figure 3b shows an isosurface plot of the net spin density for the intermediate **DR1-SiC-b**. These results are all consistent with the electronic structure of a singlet diradical species. Compared to the free reactants, both the B3LYP and the CAS calculations suggest that the diradical intermediate, **DR1-SiC-b**, is nearly thermoneutral with the free reactants. The B3LYP calculations show that the intermediate is 2.0 kcal/mol less stable than the reactants while the CAS-MCQDPT2 single point calculation gives that the intermediate is 0.3 kcal/mol more stable than the reactants. The relative free energy is 11.5 kcal/mol, this is equivalent to a 4.0 kcal/mol stabilization with respect to the preceding transition state.

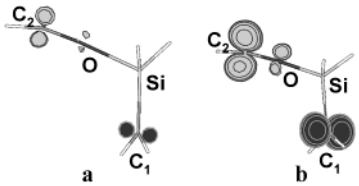

Figure 3. Isosurface plot of the net spin density of (a) the transition state **DR1-SiC-a**‡ and (b) the diradical intermediate **DR1-SiC-b**. The gray isosurface represents the α-spin density and the black isosurface the β-spin density. The isosurface value plotted is 0.02 atomic units.

Formation of the siloxetane product from the diradical intermediate can be generally described as the "swinging-in" of the formaldehyde carbon, C_2, allowing for subsequent ring closure and formation of the C_2−C_1 bond in the product. This process can be characterized by the change in the C_1−Si−O−C_2 dihedral angle from 97.7° in the intermediate, **DR1-SiC-b**, to 47.7° in the transition state, **DR1-SiC-c**‡. Analysis of the net spin densities and HOMO/LUMO occupations reveals that although the transition state **DR1-SiC-c**‡ possesses less singlet diradical character than the intermediate, it is still diradical in nature. The value of the energy barrier to product formation, obtained through the B3LYP calculations is 1.6 kcal/mol and the gas-phase free energy barrier at 298 K and 1 atm was calculated to be 2.5 kcal/mol. The CAS-MCQDPT2 single point calculations indicate that the barrier to product formation is nonexistent (activation energy of −1.5 kcal/mol). Given that the test calculations indicated that the B3LYP geometries provided a good description of the geometries of the singlet diradicals, it is likely that the transition state geometry on the CAS-MCQDPT2 potential energy surface is similar to **DR1-SiC-c**‡ on the B3LYP surface. The fact that the energies of **DR1-SiC-c**‡ are nearly thermoneutral with **DR1-SiC-b** indicate that the barrier is small and that **DR1-SiC-b** is a transient intermediate on the potential energy surface.

c(ii). Addition to Disilene and Germasilene through a Diradical Intermediate. The formation of disiloxetane (X═Y═Si) and germasiloxetane (X═Si, Y═Ge) through a diradical intermediate follow mechanisms that are similar to one another. Consequently, a general pathway applicable to both reactions will be discussed with specific details given as necessary. This pathway is distinct from that of the formation

of siloxetane (X═Si, Y═C) discussed in the previous section, and so it has been designated diradical pathway two or **DR2** in our naming scheme. The general structures of the diradical intermediates and transition states are shown in Figure 2b, whereas the energies relative to the separated reactants, B3LYP net spin densities at the radical centers, and HOMO/LUMO occupations of the CAS-MCQDPT2 natural orbitals are given in Table 3.

The separate reagents react without barrier to form a diradical intermediate, **DR2-SiY-a**, along this pathway through the formation of a Si−O bond resulting from the attack of the Si by the carbonyl group with the π-systems of the two reagents nearly perpendicular to each other. The X−O bond distance in the intermediates **DR2−SiY-a**, are within 0.01 Å of the X−O bonds in the product, thereby suggesting that the bond is fully formed in the intermediate. Once again, examination of the net spin densities at the radical centers and the HOMO/LUMO occupations shows that the electronic structure is consistent with that of a singlet diradical. It should be noted that structurally and electronically, the diradical intermediate from the addition of silene to formaldehyde, **DR1-SiC-b**, discussed in the previous subsection strongly resembles that of the diradical intermediates **DR2-SiY-a** (Y = Si, Ge). The primary difference between the two reaction pathways is that for diradical pathway 1, **DR1**, there is a barrier to formation of the intermediate from the reactants, whereas no energetic barrier for pathway 2, **DR2**, could be located.

The diradical intermediates were found to be stable with respect to the separated reactants with the energies showing a stability of 4.9 kcal/mol for **DR2-SiSi-a** (both B3LYP and CAS-MCQDPT2) and a stability of 5.6 kcal/mol for **DR2-SiGe-a** (both B3LYP and CAS-MCQDPT2). The relative free energies were 4.8 and 4.2 kcal/mol for **DR2-SiSi-a** and **DR2-SiGe-a**, respectively. Once again, they are greater than the sum of the free energies of the reactants due to a decrease in entropy of the system associated with combining the two reactants together. The reaction then has to overcome an energy barrier corresponding to a transition state, **DR2-SiY-b**‡, linking the diradical intermediate to the (di)metalloxetane products. This transition state involves the rotation of the Y-center of the Si−Y bond to allow for the subsequent closure of the four-membered ring as shown through IRC calculations. The magnitude of the barriers are small, with the values obtained through both methods showing a barrier of less than 1 kcal/mol for the formation of the disiloxetane (0.9 and 0.2 kcal/mol for B3LYP and CAS-MCQDPT2, respectively). For the barrier to form germasiloxetane, the B3LYP barrier is 0.8 kcal/mol, whereas the CAS-MCQDPT2 calculations give a negative barrier of −0.8 kcal/mol. The calculated free energy barriers at 298 K are similar to the energy barriers. For both the formation of disiloxetane and germasiloxatane, the B3LYP free energy barrier was determined to be 1.3 kcal/mol. The electronic structures of the transition states were examined in a manner similar to those of the intermediates and were found to be representative of singlet diradicals.

d. Closed-Shell Pathways. Several closed-shell stepwise and concerted pathways were located for the addition of formaldehyde to the (di)metallenes. The stepwise zwitterionic pathway for the addition to silene will be discussed in part (i). Stepwise zwitterionic pathways for the addition to digermene and disilene were located and will be discussed in part (ii). A different stepwise zwitterionic pathway for the addition to germasilene and disilene was also found and will be discussed in part (iii). Concerted pathways for the addition to silene and germene will be discussed in part (iv), and a brief discussion of the concerted pathways for the addition to disilene, germasilene, and digermene will be given in part (v).

Table 4. Energies and Bond Orders along the Zwitterionic Pathway for the Addition of formaldehyde to silene, disilene, digermene, and germasilene

	energies[a]			bond orders[b]		
species	B3LYP	CAS[c]	ΔG[d]	X–Y	X–O	C_2–O
silene X═Si, Y═C						
reactants[e]	0.0	0.0	0.0	1.82	-	1.94
ZW1-SiC-a	−1.0	−4.0	7.4	1.71	0.06	1.89
ZW1-SiC-b‡	10.8	19.6	21.2	1.19	0.37	1.48
products[f]	−49.8	−54.1	−38.8	0.8	0.64	0.91
disilene[g] X═Si, Y═Si						
reactants[e]	0.0	0.0	0.0	1.90	-	1.94
ZW2-SiSi-a	−0.2	2.9	11.0	1.26	0.27	1.77
ZW2-SiSi-b‡	2.1	3.0	11.9	1.24	0.29	1.74
products[f]	−49.2	−41.3	−38.2	0.94	0.64	0.91
digermene X═Ge, Y═Ge						
reactants[e]	0.0	0.0	0.0	1.73	-	1.94
ZW2-GeGe-a	−0.5	−4.9	9.0	1.14	0.22	1.82
ZW2-GeGe-b‡	1.8	13.3	12.3	0.93	0.35	1.60
products[f]	−25.6	−35.7	−14.5	0.91	0.63	0.94
disilene[g] X═Si, Y═Si						
reactants[e]	0.0	0.0	0.0	1.90	-	1.94
ZW3-SiSi-a	−1.0	−2.4	7.5	1.69	0.12	1.87
ZW3-SiSi-b‡	0.4	−0.1	10.1	1.52	0.21	1.78
ZW3-SiSi-c	0.4	17.0	10.1	1.19	0.38	1.56
ZW3-SiSi-d‡	4.1	16.2	14.7	0.95	0.47	1.43
products[f]	−49.2	−41.3	−38.2	0.94	0.64	0.91
germasilene X═Si, Y═Ge						
reactants[e]	0.0	0.0	0.0	1.82	-	1.94
ZW3-SiGe-a	−3.0	18.3	6.7	1.18	0.29	1.75
ZW3-SiGe-b‡	−1.6	24.2	8.3	1.20	0.30	1.72
ZW3-SiGe-c	−2.3	16.5	7.4	1.08	0.40	1.56
ZW3-SiGe-d‡	0.6	11.7	11.2	0.90	0.46	1.47
products[f]	−42.5	−34.7	−31.4	0.92	0.63	0.91

[a] Energies relative to sum of separated reactants reported in kcal/mol. [b] Wiberg bond orders. [c] CAS-MCQDPT2 single point calculations on B3LYP optimized geometries. [d] Gas phase relative free energy at 298 K and 1 atm at the B3LYP 6-311++G(d,p) level. [e] The separate (di)metallene and formaldehyde molecules. [f] The corresponding (di)metalloxetane. [g] Two distinct zwitterionic pathways were found for the addition of formaldehyde to disilene.

d(i). Addition to Silene through a Zwitterionic Intermediate. A pathway was located for the addition of formaldehyde to silene involving the initial formation of a stable intermediate resulting from nonbonding interactions between the two reactants, followed by progression through a zwitterionic transition state to yield the products. The relative energies of the stationary points along the reaction pathway, as well as relevant bonds orders are given in Table 4, whereas the structures of the intermediate and transition state are shown in Figure 4a.

A weakly bound adduct, **ZW1-SiC-a**, was found on the B3LYP potential energy surface 1.0 kcal/mol lower in energy than the reactants. The CAS-MCQDPT2 results show the energy of this species to be −4.0 kcal/mol, whereas the relative free energy is 7.4 kcal/mol. In this intermediate, the π systems of the two reactants are perpendicular to each other, which allows for the attack of the metallene by the oxygen lone pair further on along the reaction pathway. However, the Si−O bond distance in the intermediate is approximately 1.6 times the

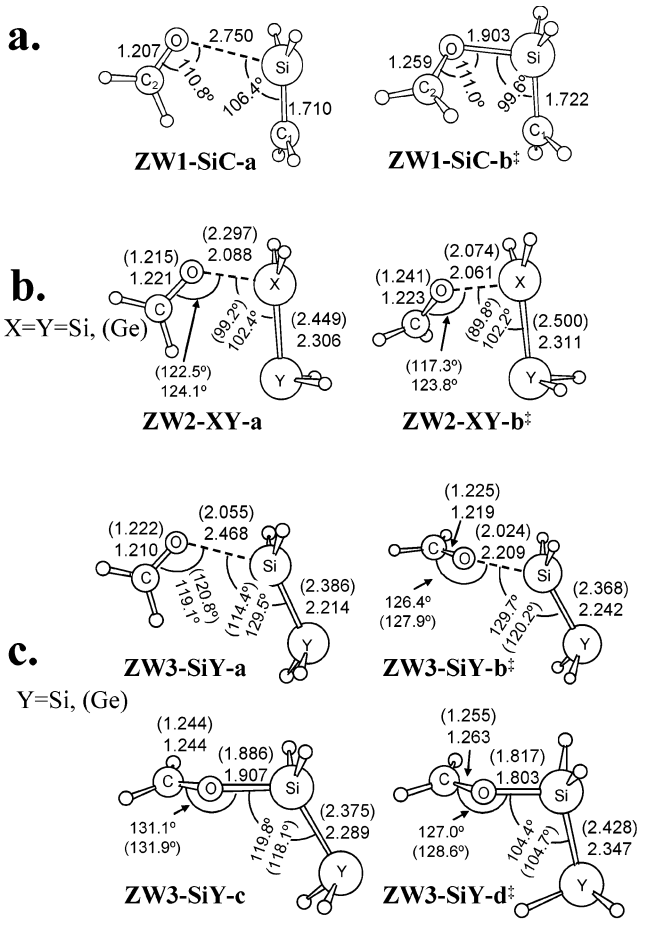

Figure 4. Geometries of intermediates and transition states along the zwitterionic pathway for the addition of formaldehyde (a) to silene, X = C, Y = Si, and (b) to disilene, X=Y=Si, and digermene, X=Y=Ge. Parenthetic parameters in (b) are for the addition of digermene. (c) Geometries of intermediates and transition states along a second zwitterionic pathway for the addition of formaldehyde to disilene, X=Y=Si, (distinct from that in (b) and to germasilene, X=Si, Y=Ge. Parenthetic parameters in (c) are for the addition of germasilene. Bond lengths are in angstroms and angles are in degrees.

distance in the product, indicating that the Si−O bond has not formed. This is further evidenced by the small Si−O Wiberg bond order of 0.06, as well as by the small changes in the bond orders of the double bonds of the two reactants. The interaction of the silene and formaldehyde moieties in **ZW1−SiC-a**, can be characterized as a weak Lewis acid/Lewis base complex, which is stabilized by the alignment of the dipoles of the two reactants.

The reaction then proceeds over an 11.8 kcal/mol energy barrier (B3LYP) connecting the intermediate to the products. The calculated free energy barrier at 298 K and 1 atm is slightly larger at 13.8 kcal/mol. The general structure of this transition state, **ZW1-SiC-b**‡, agrees with a previously reported structure for the addition to silene. The progress to products through **ZW1-SiC-b**‡ involves rotation at the carbonyl carbon, with this atom moving out of the plane defined by the four heavy atoms in the intermediate to allow for the formation of the carbon−carbon bond in the products. Examination of the HOMO and LUMO Kohn−Sham orbitals of **ZW1-SiC-b**‡ reveals a structure that is consistent with a zwitterionic species. An isosurface plot of the HOMO orbital of **ZW1-SiC-b**‡ shown in Figure 5a reveals that it can be characterized as a lone pair orbital localized on C_1, whereas the LUMO shown in Figure 5b is a π^*-like

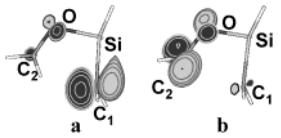

Figure 5. Isosurface plot of the (a) HOMO and (b) LUMO Kohn−Sham orbitals of the zwitterionic species **ZW1-SiC-b**‡ The isosurface value plotted is 0.1 atomic units.

orbital localized on C_2 and O. The calculated Mulliken charges are also consistent with a zwitterionic species. Specifically, the change in the Mulliken charges compared to the free reactants on C_1 are −0.22 e and +0.10 e on O.

The single point CAS-MCQDPT2 calculation provides a barrier of 23.6 kcal/mol, which is substantially larger than the B3LYP results. Because the CAS-MCQDPT2 energy is obtained using the B3LYP optimized geometry, this large energy difference might be an artifact of this procedure. This possibility was examined by changing the Si−O bond length toward both the products and the reactants, performing single point calculations at the CAS-MCQDPT2 level on these structures and evaluating the change in energy from **ZW1-SiC-b**‡. The results of this procedure reveal that small changes in the Si−O bond length at the B3LYP geometry have a large effect on the CAS-MCQDPT2 energy. For example, increasing the distance by 0.05 Å increased the energy by 6.3 kcal/mol, whereas decreasing the distance decreased the energy by 1.6 kcal/mol.

d(ii). Addition to Disilene and Digermene through a Zwitterionic Intermediate. A reaction pathway involving the formation of a zwitterionic species was also located for the addition of formaldehyde to disilene and digermene. This pathway is distinct from that discussed in the previous subsection because the intermediate can be characterized as a 1,4 zwitterionic complex. As a result, the pathway has been designated zwitterionic pathway 2 or **ZW2**. The general structures of the intermediates and transition states are shown in Figure 4b and energies and bond orders are given in Table 4.

This pathway involves the initial formation of a zwitterionic intermediate, **ZW2-XY-a**, in which the two reactants have their π-systems perpendicular to one another, allowing for the bonding interaction between the carbonyl oxygen lone pair and the X atom (X = Si or Ge). The covalent character of the X−O bond is greater in this intermediate compared to the previous zwitterionic pathway, but it is still weak. This is shown by X−O bond orders of 0.27 and 0.22 for **ZW2-SiSi-a** and **ZW2-GeGe-a**, respectively, as well as decreases in the X−Y bond order compared to that in the free dimetallene. The X−O bond distance in **ZW2-SiSi-a** and **ZW2-GeGe-a** are both 1.24 times larger than the X−O bonds in the product dimetalloxetanes. The driving force behind this interaction is the polarization of the X−Y double bond due to the presence of the carbonyl group which results in an increase in negative charge at the Y-center of the bond and an increase in the positive charge at the X-center. This was shown through natural bond analysis which revealed an occupied lone pair on the Y atom and an unoccupied lone pair orbital on the X atom. The increase of positive charge at the X-center promotes the nucleophilic attack by the carbonyl oxygen to completely form the X−O bond further along the reaction pathway.

According to the B3LYP calculations, the intermediates are only slightly more stable than the separated reactants with ΔE

= −0.2 and −0.5 kcal/mol for disilene and digermene, respectively. The multireference calculations were similar with ΔE = +2.9 and −4.9 kcal/mol for disilene and digermene, respectively. These differences are small and are likely due to differences in the minimum energy geometries on the CAS-MCQDPT2 and B3LYP potential energy surfaces. This was examined through a partial optimization of **ZW2-SiSi-a**, optimization of the bond lengths between heavy atoms, at the CAS-MCQDPT2 level which showed a 1.9 kcal/mol decrease in the energy with a very small change in bond lengths (∼0.02 Å maximum difference in bond lengths between B3LYP and CAS-MCQDPT2 structures). Presumably, if optimization of all degrees of freedom was performed, then the energy would decrease further.

The pathway then progresses over an energy barrier, **ZW2-XY-b‡**, that connects the intermediate with the products as confirmed by IRC calculations. The transition state results from the rotation of the carbonyl group out of the planar geometry formed by the four heavy atoms in the intermediate along with slight rotation at the Y atom to allow for ring closure and the formation of products. The electronic structure of **ZW2-XY-b‡** is quite similar to that of the intermediate, and the complete formation of the X−O bond has not yet occurred. The B3LYP calculations indicate that the barrier for this reaction is quite small, 2.3 kcal/mol for the addition to both compounds. The gas-phase free energy corrections to these barriers were slight with $\Delta G^{\ddagger}$(298 K) = 0.9 and 3.3. kcal/mol for the addition to disilene and digermene, respectively. The barrier determined at the CAS-MCQDPT2 level was in agreement for the addition to disilene, with a value of 1.1 kcal/mol. However, the CAS-MCQDPT2 barrier for the addition to digermene was 15.9 kcal/mol larger than the B3LYP value. To examine the underlying cause of this difference, single point calculations at the CAS-MCQDPT2 level were performed on the structures resulting from both decreasing and increasing the Y−C distance in **ZW2-GeGe-b‡** by 0.05 Å. It was observed that decreasing this distance led to a decrease in the in the barrier by 14.1 kcal/mol. The change in energy with the increase in distance was negligible. These results indicate that the difference in the barriers may result from small differences in the transition state geometries on the two potential energy surfaces.

d(iii). Addition to Germasilene and Disilene through a Zwitterionic Intermediate. A third pathway involving the formation of zwitterionic species was located for the addition of formaldehyde to disilene and germasilene. This pathway is distinctly different from the zwitterionic pathways previously discussed due to the fact that the reaction proceeds through two intermediates and two transition states in order to form the products. The pathways for the addition to both compounds are similar and thus will be discussed as a general pathway with specific data given as necessary. The structures of the various species are shown in Figure 4c, with energies and bond orders given in Table 4.

This pathway involves the initial formation of a complex resulting from a weak interaction between the Si atom and the carbonyl oxygen. In the case of disilene, the intermediate, **ZW3-SiSi-a**, can be characterized as a nonbonding adduct similar to the intermediate in zwitterionic pathway 1, **ZW1-SiC-a**. The calculated Si−O bond order is small, 0.12, and the Si−Si can still be characterized as a double bond as evidenced by the calculated bond order of 1.69. For germasilene, the first intermediate has a greater X−O covalent character as shown by the larger Si−O bond order of 0.29 and the greatly diminished Ge−Si bond order of 1.18 from 1.82 in the reactant. Despite the distinct nature of the disilene and germasilene intermediates, **ZW3-SiSi-a** and **ZW3-SiGe-a**, respectively, both are weakly bound with B3LYP binding energies determined to be 1.0 and 3.0 kcal/mol.

Direct progression from the first intermediate to the products is not possible and the reaction overcomes an energy barrier, **ZW3-SiY-b‡**, involving the rotation of the carbonyl group with respect to the dimetallene to produce a second intermediate **ZW3-SiY-c**. The value of the energy barrier is small with B3LYP values showing energies of 1.4 kcal/mol. Free energy corrections to these barriers were less than 1.2 kcal/mol with $\Delta G^{\ddagger}$(298 K) = 2.6 and 1.6 for the addition to disilene and germasilene, respectively.

This intermediate involves further formation of the Si−O bond along with the rotation of the carbonyl component with respect to the dimetallene and possesses an electronic structure consistent with a 1,4 zwitterion. For the disilene addition, the second intermediate **ZW3-SiSi-c** is almost of the same energy as the transition state **ZW3-SiSi-b‡**, with both lying 0.4 kcal/mol, above the free reactants. (**ZW3-SiSi-c** is 0.04 kcal/mol more stable.) Frequency calculations confirm that, although they are similar in energy, they are distinct stationary points and IRC calculations show that they are on the same pathway. The geometries are also distinct. For example, the Si−O bond distance in **ZW3-SiSi-b‡** is 2.209 Å while it is 0.3 Å shorter in the intermediate **ZW3-SiSi-c**. The free energies showed a stability relative to the previous transition state of 0.9 kcal/mol for the addition to germasilene, whereas the free energies of the **ZW3-SiSi-b‡** and **ZW3-SiSi-c** were equivalent.

The reaction proceeds through a second transition state corresponding to a rotation at the Y center of the dimetallene Si−Y bond to allow for subsequent ring closure to form the products. The B3LYP energies show that the second intermediate is only slightly more stable than the preceding transition state and that the barrier to the formation of products is 3.7 kcal/mol for the addition to disilene and 2.9 kcal/mol for the addition to germasilene. These results are consistent with the calculated free energy barrier of 4.6 and 3.8 kcal/mol for the formation of the products from disilene and germasilene, respectively.

A comparison of the B3LYP energies with the CAS-MCQDPT2 energies for the zwitterionic pathways reveals a number of large discrepancies. As discussed in section II-b, the B3LYP results are expected to provide accurate results for the zwitterionic pathways because all of the species involved are nearly single reference wave functions, with the ground-state determinant contributing over 95% in all cases. Although the discrepancies may be expected because the CAS-MCQDPT2 values were a result of single-point energies performed on the B3LYP geometries, the discrepancies are generally larger than those observed for the diradical pathways. To address this issue, we have performed partial geometry optimizations at the CAS-MCQDPT2 level on the intermediates. Unfortunately, full geometry optimizations and transition state optimizations could not be performed at the CAS-MCQDPT2 level. We found that **ZW3-SiSi-c** is not a minimum on the CAS-MCQDPT2 surface

Table 5. Energies and Bond Orders for Complexes along the Concerted Pathway for the Addition of Formaldehyde to Silene and Germene

	energies[a]			bond orders[b]			
species	B3LYP	CAS[c]	ΔG[d]	X–O	C_1–C_2	X–C_1	O–C_2
			silene X=Si, Y=C				
CN1−SiC‡	14.0	18.0	27.6	0.12	0.22	1.28	1.50
products[c]	−49.8	−54.1	−38.8	0.64	1.02	0.80	0.91
			germene X=Ge, Y=C				
CN1−GeC‡	16.5	13.1	27.0	0.29	0.28	1.27	1.52
products[c]	−36.7	−49.8	−25.6	0.65	1.03	0.84	0.93

[a] Energies relative to sum of separated reactants reported in kcal/mol. [b] Wiberg bond orders. [c] CAS-MCQDPT2 single point calculations on B3LYP optimized geometries. [c] The corresponding dimetalloxatene. [d] Gas phase relative free energy at 298K and 1 atm at the B3LYP 6-311++G(d,p) level.

and upon optimization attempts to dissociate progressing toward transition state **ZW3-SiSi-b**‡. Given that the B3LYP results show that **ZW3-SiSi-c** is essentially thermoneutral with the preceding transition state, it is not surprising that this intermediate is not a minimum on the CAS-MCQDPT2 potential energy surface. The partial optimizations also revealed that **ZW3-SiGe-c** was not a minimum on the CAS-MCQDPT2 potential energy surface, with the optimization taking the structure toward the products.

Partial optimizations of **ZW3-SiGe-a** revealed that the energy of this intermediate relative to that of the reactants was 1.6 kcal/mol, which is in better agreement with the B3LYP relative energy of −3.0 kcal/mol. Presumably, if all degrees of freedom were optimized, then the energy would decrease further. To examine the energy surface around **ZW3-SiGe-b**‡ single-point calculations at the CAS-MCQDPT2 level of theory were performed on structures obtained by changing the Ge−C bond length by 0.05 Å toward both the products and the reactants. The calculations showed an increase in the energy of 3.5 kcal/mol for the increase in this distance; however, for the decrease, a difference in energies of 4.4 kcal/mol was observed. This indicates that the energy of the system may be sensitive to small changes in the geometry and that the large difference in the B3LYP and CAS-MCQDPT2 energies is an artifact of performing single point calculations on the B3LYP geometry.

(iv). Concerted Addition to Silene and Germene. Pathways that were characterized as concerted additions were located for the addition of formaldehyde to silene and germene. The concerted additions to disilene, germasilene, and digermene will be discussed in the next section. The additions to silene and germene are similar and will be discussed together as a general pathway with specific information given as necessary. The relative energies of the steps along this pathway as well as relevant bond orders are given in Table 5. The general geometries of the transition state structures are given Figure 6.

For the addition of formaldehyde to germene, a concerted mechanism was the only pathway located. It was found to have a barrier of 16.5 kcal/mol at the B3LYP level of theory with the CAS-MCQDPT2 result in agreement giving a barrier of 13.1 kcal/mol. The free energy barrier for this process was larger with a value of 27.0 kcal/mol due to an addition entropic barrier. For the addition to silene, diradical, zwitterionic, and now concerted addition pathways have been located. The B3LYP barrier to the concerted addition is 14.0 kcal/mol with the CAS-MCQDPT2 energy agreeing at 18.0 kcal/mol. The free energy barrier for this addition is larger at a value of 27.6 kcal/mol.

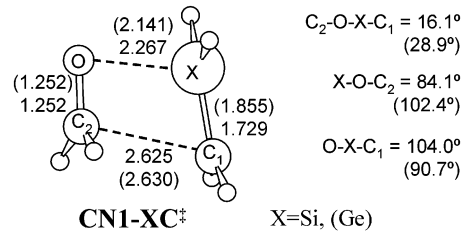

Figure 6. Geometries of transition states along the concerted pathway for the addition of formaldehyde to silene and germene. Bond lengths are in angstroms and angles in degrees. Values not in brackets are for the addition to silene (X = Si) and the bracketed values are for the addition to germene (X = Ge).

Analysis of the two transition states, **CN1-SiC**‡ and **CN1-GeC**‡ and visual inspection of the corresponding IRC pathways are consistent with a concerted process instead of a stepwise one. The bond orders reported in Table 5 show the simultaneous formation of the X−O and C_1−C_2 bonds, and breaking of the C_2−O and X−C_1 double bonds. (The C_2−O and X−C_1 Wiberg bond orders in the reactants are all in the range of 1.82−1.94).

d(v). Concerted Additions to Disilene, Germasilene, and Digermene. Many attempts to locate transition states along concerted pathways for the addition to disilene, germasilene, and digermene were made; however, no structures consistent with a concerted process were found. Either the concerted pathways do not exist on the B3LYP potential surface or we could simply not find them. To address the latter possibility, an estimate of the energetics of concerted mechanisms for the addition of formaldehyde to disilene, germasilene, and digermene was determined. A linear transit procedure was employed at the B3LYP level in which the X−O and Y−C distances were constrained such that the ratio of these two distances was equal to the same ratio in the products at each step along the reaction pathway, whereas all other degrees of freedom were optimized. This was performed to simulate the simultaneous formation of the X−O and Y−C bonds. It was observed that the B3LYP energies at the roughly located transition states relative to the sum of the energies of the reactants were 10.4, 6.6, and 8.3 kcal/mol (without zero-point energy correction) for the additions to disilene, germasilene, and digermene, respectively. These rough concerted energy barriers are much higher than the barriers found for the other pathways located for these addition reactions and as a result they were not further explored.

e. Solvent Effects. The results discussed above have been generated from gas-phase simulations. However, one might expect more polar solvents to stabilize the zwitterionic pathways more so than the concerted or diradical addition pathways. We have explored the effect of solvent on the gas-phase reaction pathways previously discussed using the polarizable continuum model (PCM). More specifically, we have performed single-point PCM calculations at the B3LYP/6-311++G(d,p) level using the gas-phase geometries on all reactants, products, intermediates, and transition states for the additions to silene, disilene, and germasilene. The solvation calculations we have performed can be considered qualitative in nature. They will suggest trends and to a degree how strong the solvation effects may be. The results of the PCM calculations are shown in Table 6, for the following solvents: cyclohexane, acetone, acetonitrile

Table 6. Energies for the Reaction of Silene, Disilene and Germasilene with Formaldehyde in the Presence of Solvents

		calculated relative energy[a] in			
species	gas-phase	cyclohexane	acetone	acetonitrile	water
		silene			
DR1-SiC-a‡	5.5	5.6	(4.3)[b]	(4.2)[b]	(4.1)[b]
DR1-SiC-b	2.0	3.5	5.8	5.9	6.0
DR1-SiC-c‡	3.6	5.1	7.4	7.6	7.7
ZW1-SiC-a	−1.0	−0.4	0.4	0.4	0.5
ZW1-SiC-b‡	10.8	11.1	11.4	11.4	11.4
CN1-SiC‡	14.0	14.7	15.6	15.7	15.7
products	−49.8	−48.7	−46.9	−46.8	−46.7
		disilene			
DR2-SiSi-a	−4.9	−3.5	−1.7	−1.6	−1.5
DR2-SiSi-b‡	−4.0	−2.6	−0.6	−0.5	−0.4
ZW2-SiSi-a	−0.2	1.0	0.6	0.6	0.6
ZW2-SiSi-b‡	2.1	0.9	0.4	0.3	0.3
ZW3-SiSi-a	−1.0	−1.0	−0.7	−0.7	−0.6
ZW3-SiSi-b‡	0.4	−0.2	−1.1	−1.2	−1.0
ZW3-SiSi-c	0.4	−0.2	−1.7	−1.8	−1.9
ZW3-SiSi-d‡	4.1	3.8	2.5	2.4	2.3
products	−49.2	−48.3	−47.2	−47.1	−47.1
		germasilene			
DR2-SiGe-a	−5.6	−4.2	−2.3	−2.2	−2.1
DR2-SiGe-b‡	−4.8	−3.4	−1.4	−0.6	−1.2
ZW3-SiGe-a	−3.0	−4.8	−7.2	−7.3	−7.4
ZW3-SiGe-b‡	−1.6	−3.4	−5.9	−6.1	−6.2
ZW3-SiGe-c	−2.3	−3.5	−5.6	−5.8	−5.9
ZW3-SiGe-d‡	0.6	−0.2	−2.1	−2.3	−2.4
products	−42.5	−41.5	−40.0	−39.9	−39.8

[a] Energies kcal/mol relative to the sum of the energies of the separated reactants calculated at the B3LYP/6-311++G(d,p) level with the PCM solvation model. Zero-point corrections equal to those calculated in the gas-phase added to all energies. [b] Using the PCM solvation model, these intermediates no longer possessed diradical character.

and water, which have dielectric constants of 2.02, 20.70, 36.64, and 78.39, respectively. Although experimentally these reactions are not likely to be performed in water or acetone due to the fact that competitive reactions with the solvent could occur, this choice of solvents was used to examine a wide range of solvent dielectric constants. (In the PCM simulations, the solvent molecules are not treated explicitly.) We note that these reactions have experimentally been performed in hexanes[47−49] and acetonitrile.[40] The effect of solvents on the reactions with germene and digermene were not performed because only one mechanistic pathway was located for these additions.

e(i). Solvent Effects—Addition to Silene. On the basis of the gas-phase calculations presented above, the diradical pathway was favored over both a zwitterionic and concerted addition mechanism. The results of the solvation simulations are given in Table 6. The most apparent difference is that the transition state, **DR1-SiC-a‡**, linking the reactants to the diradical intermediate, **DR1-SiC-b**, is lower in energy than the diradical intermediate for all solvents considered except cyclohexane. This is possible because we have only performed single point solvation calculations on the gas-phase geometries. Thus, the single point geometries are not stationary points in the solvation calculations. However, further examination of the electronic structure of **DR1-SiC-a‡**, revealed that this species no longer possessed diradical character in all solvents except cyclohexane. Thus, it was not representative of the diradical path resulting in the anomolous results.

In all of the solvents considered, the zwitterionic intermediate is more stable than the diradical intermediate and the concerted pathway is always highest in energy, as in the gas-phase calculations. As the polarity of the solvent increases (i.e., dielectric constant increases), the barrier from the diradical intermediate to the products remains constant, however the energies of **DR1-SiC-b** and **DR1-SiC-c‡** relative to the energy of the reactants increases. The barrier to product formation through a zwitterionic intermediate decreases by 0.6 kcal/mol as the polarity of the solvent increases along with a decrease of 0.9 kcal/mol in the stability of the intermediate with respect to the reactants. As a result, the zwitterionic intermediate becomes slightly more preferred with respect to the diradical as the polarity of the solvent increases, a trend that is expected. The amount of this stability is minimal and thus as in the gas-phase both the zwitterionic and diradical pathways are competitive.

e(ii). Solvent Effects—Addition to Disilene. The results of the gas phase calculations for the addition of formaldehyde to disilene indicated that the pathway involving the formation of a diradical intermediate is preferred. The other two pathways found were zwitterionic in nature and as a result may be stabilized by polar solvents. The results of the solvation calculations show that in the presence of a nonpolar solvent such as cyclohexane the diradical pathway is still clearly favored. This is an important result because the experiments involving the addition of mechanistic probes to disilenes which resulted in the proposal of a diradical mechanism were performed in hexanes.[47,48] However, as the polarity of the solvents increases the diradical intermediate and transition state becomes destabilized with respect to the reactants by up to 3.6 kcal/mol (gas-phase to water), whereas the relative energies of the zwitterionic complexes change by −2.3 to +1.8 kcal/mol. As a result, the difference in energies between the diradical and the zwitterionic pathways decreases as the polarity of the solvent increases as would be expected. The diradical pathway still remains the most favorable even in the presence of the most polar solvent consider (water); however, in this solvent, pathways **DR2** and **ZW3** are similar in energy with the exception of the barrier to the products which is 4.2 kcal/mol for the zwitterionic pathway, but only 1.1 kcal/mol for the diradical pathway.

e(iii). Solvent Effects—Addition to Germasilene. From the gas phase results presented above, it was clear that the diradical pathway was favored over the zwitterionic pathway for the addition of formaldehyde to germasilene. In the presence of cyclohexane, the diradical pathway is still favored, which agrees with the results of the addition of mechanistic probes to germasilenes in hexanes. However, in the presence of more polar solvents, the solvation simulations suggest that the addition of germasilene will favor the zwitterionic pathway even for acetone. As the polarity of the solvent increases, the zwitterionic pathway becomes increasingly favored, with all steps along this pathway being lower in energy than the diradical pathway for all solvents considered except cyclohexane. Thus, the addition reaction involving germasilene is more strongly affected by solvent than disilene, favoring a zwitterionic pathway in polar solvents.

f. Pathway Selectivity. It is interesting to note from the results presented above that there are fewer pathways available for the addition of formaldehyde to germene and digermene than there are for the other three (di)metallenes studied. In particular, no mechanisms involving the formation of diradical intermediates were available for the reaction of formaldehyde with germene and digermene. In other words, when a Ge−O

bond is formed during the reaction the diradical pathway is not observed, whereas when a Si−O bond is formed the diradical pathway is available. Because the zwitterionic pathways involve charge-polarized intermediates, it is possible that the selectivity may be due to the polarizability of silicon versus germanium. However, both elements have similar atomic polarizabilities.[90] As previously discussed, the diradical pathways involve the formation of intermediates in which Si−O covalent bond is fully formed and where the bond lengths are essentially the same (within 2%) distance as in their respective products. On the other hand, the intermediates along the zwitterionic pathways have weak X−O bonds, with X−O bond distances that are 12−45% larger than that in their respective products.

We suggest that a major contributing factor to the observed pathway selectivity is a result of the decreased thermodynamic stability of the Ge−O bond in comparison with the Si−O bond. When X = Si, the strong Si−O bond stabilizes the diradical intermediate whereas when X = Ge, the Ge−O bond is not strong enough stabilize the intermediate. Because the X−O bonds in the zwitterionic intermediates are weak, these species do not exhibit the same destabilization as the diradical species and the formation of zwitterionic complexes with both Si−O and Ge−O bonds is possible.

To test this hypothesis, it is necessary to have bond energies for the Si−O and Ge−O bonds. Experimental values for both bond energies are available with those for Si−O ranging from 122.4 to 136.0 kcal/mol[68] and those for the Ge−O ranging from 72.0[91] to 107.0[92] kcal/mol. It is apparent that the Si−O bond is stronger; however, given that the ranges of these values, particularly for the Ge−O bonds, are large it was decided to calculate the bond energies to better determine the difference in the energy between the two bonds. Thus, the bond energies were calculated through a series of dehydrogenation thermochemical cycles as outlined in the Computational Details and Scheme 2. This technique has previously been employed to evaluate π-bond energies of (di)metallene systems.[82,84,93]

The results of the calculations revealed Si−O bond energies of 118.9, 117.1, and 116.3 kcal/mol for the addition to silane, disilane, and germylsilane, respectively. This corresponds to an average calculated Si−O bond energy of 117.4 kcal/mol, slightly lower than the range of values given above. The bond energy of the Ge−O bond was found to be 99.1 and 96.8 kcal/mol for the reaction of methanol with germane and digermane, respectively. This results in an average Ge−O bond energy of 98.0 kcal/mol. This value falls within the range of the reported Ge−O bond dissociation energies given above.

These calculations indicate that the Ge−O bond is approximately 19 kcal/mol weaker than the Si−O bond. An examination of the diradical reaction pathways discussed above shows that the intermediates along these pathways are only slightly more stable than the reactants, on the order of only a few kcal/mol if an Si−O bond is formed. If the mechanism involves the formation of a Ge−O bond, then the intermediate would no longer be energetically favored and dissociation to form the reactants would occur. This is indeed what was observed upon attempting to locate diradical intermediates for the reaction of formaldehyde with germene and digermene and as a result of this difference in bond energies these (di)metallenes are limited in the number of reactive pathways available to them. We have additionally examined the addition of germasilene to formaldehyde in which the Ge−O bond forms instead of the more favored Si−O bond. (Recall that a favorable diradical pathway is found for this addition when the Si−O forms.) All attempts to locate such a diradical intermediate lead to a zwitterionic complex, a result that agrees with the idea that the strength of the X−O bond influences the pathway selectivity.

For the addition reactions involving silene, disilene, and germasilene, both diradical and zwitterionic pathways are available. It is interesting to consider what determines the pathway selectivity because the interaction between the reactant molecules reacting along the diradical and zwitterionic pathways is similar, resulting in the formation of intermediates possessing O−X bond. The answer to this question may lie in how the two reactant molecules approach one another to proceed through either the zwitterionic or diradical pathways. In the approach leading to the zwitterionic pathways, the formaldehyde and dimetallene molecules approach one another with their π systems perpendicular allowing for the interaction of the carbonyl oxygen nonbonding-orbital with the π^* orbital of the (di)metallene. In this approach the C−O−X−Y dihedral angle is very close to 0° as shown in Figure 4, and hence, the dipole of the formaldehyde is aligned with X−Y bond which may induce some polarization of this bond facilitating the formation of the zwitterionic species. Additionally, in this orientation the two ionic centers, the carbon of formaldehyde and the Y center of the (di)metallene, are in closer proximity to one another, upon comparison with the diradical species, offering stability to the zwitterion. The approach that results in the diradical species is different than that just described for the zwitterionic pathway particularly with the C−O−X−Y dihedral angle being much larger at ∼90°. Hence, the dipole of the carbonyl species is perpendicular to the X−Y bond and polarization of this bond is not induced. In this arrangement, the distance between the carbonyl carbon and the Y-center of the (di)metallene is also much larger than that in the zwitterion and electrostatic stabilization of any charge accumulation at these centers would be much less.

Related to the question of pathway selectivity, the ease in which the reactants can switch between diradical and zwitterionic pathways during the course of the reaction is of interest. This is of particular significance in the case of silene because the zwitterionic intermediate, **ZW1-SiC-a**, is lower in energy than the diradical intermediate, **DR1-SiC-b**, but the reaction barrier to the products along the zwitterionic pathway is larger than that of the diradical pathway (see Figure 7a). Thus, a possible low energy reaction channel for the addition of formaldehyde to silene may first involve the initial formation of the zwitterionic intermediate, **ZW1-SiC-a**, followed by a transition to the diradical pathway to form a diradical species such as **DR1-SiC-b**. To explore this possibility, a potential energy surface scan has been performed by decreasing the Si−O distance from that in **ZW1-SiC-a** to that in **DR1-SiC-b** in increments of 0.1 Å and optimizing the remaining degrees of freedom at the B3LYP/6-311++G(d,p) level of theory. It was observed that a smooth transition was made from the zwitter-

(90) *CRC Handbook of Chemistry and Physics*, 81 ed.; Lide, D. R., Ed.; CRC Press: Boca Raton, London, New York, Washington, DC, 2000.
(91) Shaulov, Y. K.; Federov, A. K.; Zueva, G. Y.; Borisyuk, G. V.; Genchel, V. G. *Russ. J. Phys. Chem. Engl. Ed.* **1970**, *44*, 1181.
(92) Jackson, R. A. *J. Organomet. Chem.* **1979**, *166*, 17.
(93) Schmidt, M. W.; Truong, P. N.; Gordon, M. S. *J. Am. Chem. Soc.* **1987**, *109*, 5217.

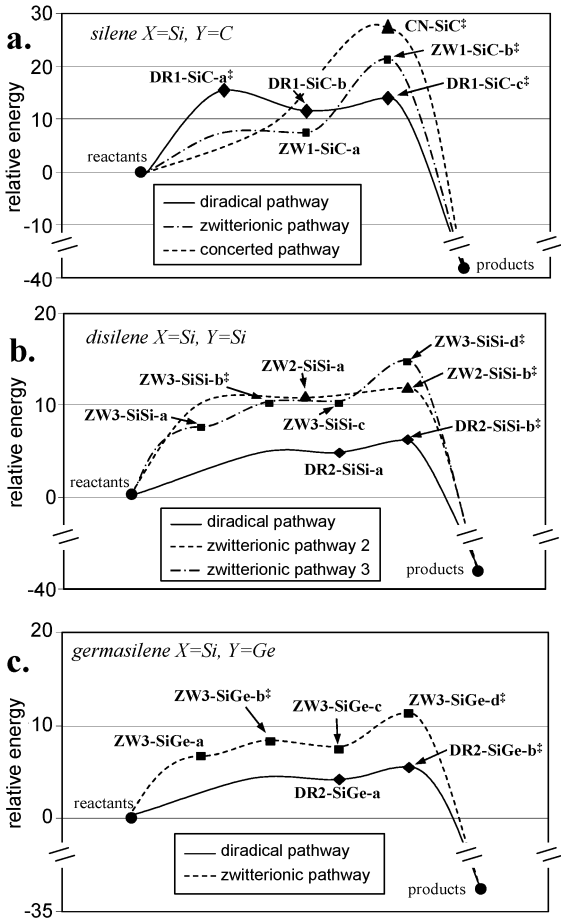

Figure 7. (a) B3LYP gas-phase free energy profiles at 298 K and 1 atm for the addition of formaldehyde to (a) silene, (b) disilene, and (c) germasilene. Energies are in kcal/mol relative to the sum of the energies of the separated reactants.

ionic to diradical intermediate with the highest energy point along this coordinate being equivalent to an estimated activation energy of 6.5 kcal/mol. Transition state optimization of the highest energy structure along this path yielded **DR1-SiC-a**‡, which was shown by IRC calculations not to connect **ZW1-SiC-a** to **DR1-SiC-b**. We were unable to locate a formal transition state for this process by any other means. However, to further estimate the energetic requirements of the transition from the zwitterionic to diradical pathways structure **DR1-SiC-b** was forced to adopt a closed-shell electronic structure. The energy of this closed shell species was such that an approximate barrier of 17.8 kcal/mol is estimated for the process: **ZW1-SiC-a** to **DR1-SiC-b(closed-shell)** to **DR1-SiC-b(open-shell)**. Although **ZW1-SiC-a** and **DR1-SiC-b** are displayed close to one another in Figure 7a, the transition between the zwitterionic and diradical pathways may involve different species. Thus, an analogous set of calculations were performed to consider the process: **ZW1-SiC-a** to **DR1-SiC-a**‡(closed-shell) to **DR1-SiC-a**‡(open-shell). The estimated barrier for this process is only 7.0 kcal/mol. Thus, a reaction channel involving the transition from a zwitterionic intermediate to the diradical pathway may be competitive with the purely zwitterionic and diradical pathways for the addition reaction involving silene.

IV. Summary and Comparison to Experiment

A comparison of the pathways described above for the addition of formaldehyde to each (di)metallene is presented in sections a to e and the most likely mechanistic pathway based on the results is proposed along with comparison to experimental results. To present our results clearly, only the free energies at 298 K and 1 atm are shown in Figure 7. The B3LYP and CAS-MCQDPT2 results will be discussed as necessary although they provide the same qualitative description of the reaction pathways as the free energies. The conclusions are given in part f.

a. Addition to Germene. The calculations indicated that for the addition of formaldehyde to germene, the only pathway for the formation of germoxetane is that involving progression through a concerted transition state as previously discussed in section III-d(iv). It is interesting to note that this pathway was the only one located for the addition to germene, and thus, it appears that germene does not react with formaldehyde in a similar manner as silene which has several paths available for the formation of products. As stated in the Introduction the elucidation of the mechanism of the addition to germenes has not received much attention; however, a transition state of a similar geometry has been located through previous B3LYP calculations.[50] Our results are consistent with the existing kinetic data.[41,94] No detectable reaction was reported for the addition of acetone to 1,1-diphenylgermene[41] in agreement with our finding that there are no low lying pathways available for the addition of formaldehyde to germene. However, a reaction was detected in the addition of acetone to a (1-germa)hexatriene[94] suggesting that a change in substituents may make a stepwise pathway accessible (presumably involving a biradical by comparison to the silene system.[42])

b. Addition to Digermene. Only one reaction pathway, a stepwise zwitterionic process, was located for the addition of formaldehyde to digermene with a calculated free energy barrier of 3.3 kcal/mol from the intermediate to the products. Although an estimated barrier for a concerted reaction has been calculated at 10−11 kcal/mol (at the B3LYP level), no formal stationary points could be located for the pathway. This estimated barrier is approximately 8 kcal/mol greater than the barrier to the zwitterionic process. Thus, we conclude that the most likely pathway for the addition of formaldehyde to digermene occurs through the formation of a zwitterionic intermediate and transition state as discussed in section III-d(ii). This is an interesting conclusion given that it had previously been proposed that the addition occurred through a concerted process.[49] We note, however, that this result was drawn from experiments that ruled out the possibility of diradical intermediates, but were not able to distinguish between zwitterionic or concerted mechanisms.[49] The fact that a diradical pathway was not found is in agreement with experiments.

c. Addition to Silene. For the addition of formaldehyde to silene three competing pathways were located involving the formation of either diradical or zwitterionic species or progression through a concerted transition state. A comparison of the free energies of these pathways is shown in Figure 7a. The B3LYP and CAS-MCQDPT2 calculations given in Tables 3, 4, and 5 are in qualitative agreement with the free energies. The free energy profiles show that the diradical and zwitterionic

(94) Leigh, W. J.; Toltl, N. P.; Apodaca, P.; Castruita, M.; Pannell, K. H. *Organometallics* **2000**, *19*, 3232.

pathways are competitive. The estimated free energy barrier for the formation of the intermediate **DR1-SiC-b** along the diradical pathway is 15.5 kcal/mol, whereas the free energy barrier for product formation from the zwitterionic intermediate, **ZW1-SiC-a**, is 13.8 kcal/mol. Our calculations suggest that the concerted pathway which has a free energy barrier of 27.0 kcal/mol from the reactants is not competitive with the zwitterionic and diradical pathways. As detailed in section III-f, "Pathway Selectivity", the possibility of a hybrid reaction channel involving the initial formation of the zwitterionic intermediate **ZW1-SiC-a**, followed by a transition to the diradical pathway may also be operative. Here, we have estimated an overall energy barrier of 7.0 kcal/mol. Because no formal transition states could be located for this process, this value is a zero-temperature electronic energy barrier that does not include zero-point energy corrections, not a finite temperature free energy barrier. Thus, to be put on equal footing with the purely diradical and purely zwitterionic pathways, the 7.0 kcal/mol barrier for the hybrid reaction channel must be compared to the 4.16 kcal/mol overall barrier for the diradical pathway and the 11.5 kcal/mol overall energy barrier for zwitterionic pathway.

Experimentally, all three mechanisms (diradical, zwitterionic, and concerted) have been implicated for the addition of carbonyls to silene.[27,40,42,45,46,95] Our results slightly favor the zwitterionic pathway over the diradical pathway. Furthermore, the solvation calculations suggest that the zwitterionic pathway is more favored as the polarity of the solvent increases. Because the zwitterionic and the diradical pathways are competitive, substituent effects may play a large role in ultimately determining which pathway is favored. This is consistent with the varied experimental results showing diradical and zwitterionic pathways depending on the reaction conditions and reactants. The calculations presented here are not consistent with the observation of a concerted mechanism—a result that is in agreement with most experimental studies.[96]

d. Addition to Disilene. Three pathways, two involving the formation of zwitterionic species and one involving the formation of diradical structures were located for the addition of formaldehyde to disilene. A comparison of the free energies along the three stepwise pathways is shown in Figure 7b. The energy barrier of a concerted process was estimated; however, a transition state was not located and thus the data are not shown. This comparison demonstrates that the pathway involving the formation of diradical species is clearly most energetically favorable, with all steps along the diradical pathway being lower in energy than the reactants. This is also true in all solvents considered in this study. The B3LYP and CAS-MCQDPT2 results, although not presented in Figure 7b, also indicate that the diradical pathway is significantly lower in energy than the other mechanisms. These findings agree with the previous proposals,[47,48] based on studies with mechanistic probes, that the addition to disilene occurs through a diradical intermediate.

e. Addition to Germasilene. Shown in Figure 7c is the calculated gas-phase free energy pathways for the addition of formaldehyde to germasilene at 298 K. One pathway involves the formation of zwitterionic species and another involving the formation of diradical species. The barrier for a concerted process was estimated, however, a transition state for a concerted pathway was not located. The comparison of the free energy pathways shown in Figure 7c shows that the diradical mechanism is favored over the zwitterionic mechanism in the gas phase. Experimental studies[47,48] in hexane with mechanistic probes show evidence of a diradical intermediate, which agrees with our gas-phase results. Our solvation simulations, suggested that in all solvents more polar than hexane, the zwitterionic pathway was favored. Thus, we suggest that similar mechanistic studies performed in more polar solvents may not show evidence of a diradical intermediate.

V. Conclusion

We have examined the addition of formaldehyde to silene, disilene, germene, digermene, and germasilene in an effort to provide fundamental knowledge of the mechanistic pathway for the addition of nonenolizable aldehydes and ketones to (di)-metallenes. Attempts were made to locate pathways involving both closed- and open-shell species, as well as concerted processes, to allow for a comparison of these paths through theoretical means. It was found that for the addition of formaldehyde to germene the only pathway available is a concerted one. For the addition to digermene a stepwise zwitterionic pathway was located and found to be more favorable than the estimated concerted process. For the addition of formaldehyde to silene, zwitterionic, diradical, and concerted pathways were located, with the zwitterionic and diradical paths being quite similar in energy in the gas phase. For the additions to disilene and germasilene, it is clear that the diradical pathway is energetically favored in the gas phase, although pathways involving the formation of species with zwitterionic electronic structures were also found.

Our calculations reveal that when a Ge−O bond forms during the addition, a diradical pathway is not available, whereas when a Si−O bond forms during the addition, both diradical and zwitterionic pathways are found. We find that the distinct nature of the X−O (X = Si or Ge) bond in the zwitterionic and diradical intermediates, as well as the difference in the bond energies of the Si−O (∼117 kcal/mol) and Ge−O (∼98 kcal/mol) bonds play a significant role this pathway selectivity. In the diradical intermediates, the X−O covalent bond is fully formed, whereas in the zwitterionic intermediates it is signficantly weaker. Therefore, for the addition of silene, disilene and germasilene in which a Si−O bond forms the diradical intermediate is stabilized by the strong Si−O bond and a diradical pathway is available. On the other hand, for the addition of germene and digermene where a Ge−O bond forms, the weaker Ge−O bond is not strong enough to stabilize the diradical intermediate and therefore the diradical pathways are not observed in those cases. A significant difference is noted between the pathways available to the metallenes in comparison to the dimetallenes. Specifically, a concerted pathway is available to silenes and germenes but not to disilene, digermene, and germasilene. This may be due to the fact that silene and germene have a more polarized X═Y double bond than disilene, digermene, and germasilene (Ge and Si are close in electronegativity). However, we have not explored this further. We also note that the concerted reaction channels for disilene, digermene, and germasilene may exist but we could not locate formal transition states for them.

(95) Leigh, W. J.; Sluggett, G. W. *Organometallics* **1994**, *13*, 1005.
(96) An early kinetic study by Leigh and co-workers[43] provided evidence which was interpreted in terms of a concerted addition of acetone to 1,1-diphenylsilene; however, subsequent studies favor a zwitterionic pathway.[23]

Solvation simulations were performed to examine the effect of solvent polarity on the reaction energetics. The solvents cyclohexane, acetone, acetonitrile, and water, which cover a wide range of dielectric constants, were simulated. The solvent simulations showed that the diradical and zwitterionic pathways remain similar in energy for the addition to silenes even in the presence of polar solvents. The addition of formaldehyde to disilene is slightly more sensitive to solvent effects, but the diradical pathway is still favoured over the range of solvent polarities examined. The addition involving germasilene is the most sensitive to solvent polarity. The diradical pathway is favored only in the most nonpolar solvent tested (cyclohexane). In the presence of polar solvents, the zwitterionic pathway is favored, and becomes more favored as the solvent polarity increases.

The results of the current study provide valuable insight into the nature of the pathways for the addition to these (di)-metallenes and although the (di)metallenes considered in this study are not observed in chemical reactions, their examination provides a basis for the explanation of experimental findings with regards to the mechanism of nonenolizable aldehyde and ketone addition to (di)metallenes.

Acknowledgment. We gratefully acknowledge the Natural Sciences and Engineering Research Council of Canada (NSERC), the Canada Foundation for Innovation, the Ontario Innovation Trust, and the Academic Development Fund at the University of Western Ontario for financial support. Computing resources made available by SHARCnet of Canada is also acknowledged.

Supporting Information Available: Cartesian coordinates and total energies of all optimized stationary points. A detailed description of the active space used in the CAS-MCQDMPT2 calculations. This material is available free of charge via the Internet at http://pubs.acs.org.

JA0269845